

Plasticity Neural Network Based on Memory Generation-Consolidation-Loss and Synaptic Strength Rebalance by Current and Memory Brain Plasticity and Synapse Formation to simulate Artificial Brain

Jun-Bo Tao^{1,**}, Bai-Qing Sun^{2,**}, Wei-Dong Zhu³, Shi-You Qu^{4,**},
Ling-Kun Chen⁵, Jia-Qiang Li⁶, Guo-Qi Li⁷, Chong Wu^{8,*}, ,
Yu Xiong^{9,*}, and Jiaxuan Zhou¹⁰

¹Ph. D. candidate, School of Management, Harbin Institute of Technology, Harbin, Heilongjiang 150001, China. Email: 17B918053@stu.hit.edu.cn

²Ph. D., School of Management, Harbin Institute of Technology, Harbin, Heilongjiang 150001, China. Email: baiqingsun@hit.edu.cn

³Ph. D., Department of Mechanical Engineering University of Maryland, Baltimore County, Baltimore, MD 21250, U.S.A. Email: wzhu@umbc.edu

⁴Ph. D., School of Management, Harbin Institute of Technology, Harbin, Heilongjiang 150001, China. Email: qushiyou@hit.edu.cn

^{5a}Ph. D., College of Civil Science and Engineering, Yangzhou University, Yangzhou,

^{5b}Jiangsu 225127, China; Email: lingkunchen08@hotmail.com

^{5c}Department of Civil and Environmental Engineering, University of California, Los Angeles, CA 90095, USA School of Civil Engineering, Southwest Jiaotong University, Chengdu, 610031 Sichuan, China

⁶Ph. D., Institute No.25 of the Second Academy China Aerospace Science and Industry Corporation Limited, Beijing 100048, China. Email: lijiaqiang1988926@126.com

^{7a} Institute of Automation, Chinese Academy of Science, Beijing, 100190, China. Email: guoqi.li@ia.ac.cn

^{7b} University of Chinese Academy of Science, Beijing, 100049, China

⁸Ph. D., School of Management, Harbin Institute of Technology, Harbin, Heilongjiang 150001, China. Email: nmem2022@outlook.com

⁹Ph. D., Surrey Business School, University of Surrey, Guildford, Surrey GU2 7XH, United Kingdom. Email: y.xiong@surrey.ac.uk

¹⁰School of Management, Harbin Institute of Technology, Harbin, Heilongjiang 150001, China. Email: 1191000315@stu.hit.edu.cn

* Correspondence and requests for materials should be addressed to Chong Wu (email: nnem2022@outlook.com) and Yu Xiong(email: y.xiong@surrey.ac.uk)

**These authors contributed to the work equally and should be regarded as co-first authors.

Keywords: Deep learning; Synaptic strength rebalance; Synaptic competition; Constant synaptic effective range; Random synaptic effective range; Optimization synaptic effective range; PNN; RNN; BP; Computational neuroscience; current and memory brain plasticity; Current gradient information; Memory negative and positive gradient information; Astrocytic synapse formation cortex memory persistence factor; Astrocytes phagocytose synapses factor; Critical period; Memory engram cells; Retrograde retrieval memory; Quantum computing; Brain dynamics; Alzheimer’s disease

In brief: The mechanism of our proposed Neural Network (NN) is very well in line with the results of the latest MIT brain plasticity study, in which researchers found that as a synapse strengthens, neighboring synapses automatically weaken themselves to compensate [14]. Nevertheless, our neural network treats synapses as a group of intelligent agents to achieve synaptic strength rebalance. And Dr. Luo’s team at Stanford University has put forward that competition regarding synapse formation for dendritic morphogenesis is crucial, also reflected PNN simulates synapse formation [15]. The paper’s analysis suggests retrograde mechanism, was reflected in PNN through retrograde retrieval memory [16]. The decrease of neurogenesis was considered throughout aging. And PNN simulates synapse formation, decrease of neurons at the same time [17]. But controversy was claimed that human hippocampal neurogenesis persists throughout aging, PNN considered it may have a new and longer circuit in late iteration [18]. We try to conduct research on the mechanism of failure in brain plasticity by model at the closure of critical period in details by contrasting with studies before [19]. By simulations, the PNN gave the two cases with and without negative cortex memories persistence. And the paper proposed $\alpha 7$ -nAChR-dependent astrocytic responsiveness is an integral part of the cellular substrate underlying memory persistence by impairing fear memory[20]. The effect of astrocyte made local synaptic effective range remain in an appropriate length at critical period[21]. Both negative and positive memories can be reflected in brain cortex, and its simulations fits very well with experiments in the relationship of human intelligence and cortical thickness, individual differences in brain[22]. PNN also considered the memory engram cells that strengthened synaptic strength[23]. And paper found that

1064-nm Transcranial photobiomodulation (tPBM) applied to the right prefrontal cortex (PFC) improves visual working memory capacity[24], the effect of PNN (memory structure) may be the same with smaller losses in signals. The Dr. Christian Kerskens and David López Pérez suggests consciousness is non-classical [25], so PNN introduces exacted memory brain plasticity by quantum computing in retrograde mechanism, non-classical working memory brain plasticity, in extracted relatively good or inferior memories brains plasticity will exhibit exponential decay of wave function for a while because of barriers. The research group of Rockefeller University propose a thalamo-cortical circuit that gates memory consolidation, and suggest the selection and stabilization of hippocampal memories into longer-term cortical storage[26]. Researchers found that efficient information transmission of the brain relies on turbulence[27]. So short-term memory turns long-term memory due to the laminar-turbulent transition.

The paper suggest that impaired MCH-system function contributes to aberrant excitatory drive and sleep defects, which can compromise hippocampus-dependent functions [28]. And energy loss of hippocampus might change the gradient direction of cognitive search.

Through the PNN tests, we found that the astrocytic cortex memory persistence factor, like the astrocytes phagocytose synapses factor, produces the effect of reducing the local accumulation of synapses. Considering both negative and positive cortex memories persistence help activate synapse length changes. In the calculation to update the synaptic effective range, the PNN in which only the effect of astrocytes phagocytose synapses is considered regardless of the gradient update, proves simple and effective.

Positive or negative working memory or short-term memory brain plasticity is quantum, and exhibits exponential decay of wave function for a while, produced in the hippocampus. And exponential decay because of barriers, and barriers may relate to astrocytes. Working memory brain plasticity goes through brain from hippocampus to cortices by directional derivative. The strong working memory brain plasticity turns to long-term memory means maximum of directional derivatives, that is gradient. So long-term memory means gradient of working memory brain plasticity. Similarly, memory flows to the n th external cortex may be the n th derivative of brain plasticity. Is it possible to reduce the number of animal experiments and their suffering by simulating and planning the factors of biological experiments through Deep learning?

Summary: Beyond the consideration of the basic connection, this research focuses on a new Neutral Network (NN) model, referred as PNN (Plasticity Neural Network) in which the current and memory effective range between synapses and neurons plastic changes with iterations, are both taken into account at the same time, specifically, the current and memory synaptic effective range weights.

In addition, this mechanism of synaptic strength rebalance is consistent with the findings in the recent research on brain plasticity at the MIT Picower Institute. Regarding the importance of this mechanism [14], our Neural Network is, it treats synapses as a group of intelligent agents to achieve synaptic strength rebalance. Dr. Luo’s team at Stanford University has mentioned that the competition regarding synapse formation for dendritic morphogenesis is important, also reflected PNN simulates synapse formation[15]. We try to examine the mechanism of failure in brain plasticity by model at the closure of critical period in details by contrasting with studies before[19].

The PNN model is not just modified on the architecture of NN based on current gradient informational synapse formation and brain plasticity, but also the memory negative and positive gradient informational synapse formation and memory brain plasticity at critical period. By simulations, the PNN gave the two cases with and without negative cortex memories persistence. And the paper proposed $\alpha 7$ -nAChR-dependent astrocytic responsiveness is an integral part of the cellular substrate underlying memory persistence by impairing fear memory[20]. In addition, memory brain plasticity involves the plus or minus disturbance-astrocytes phagocytose synapses factor, through which the synaptic homeostasis is achieved[21]. The effect of astrocyte made local synaptic effective range remain in an appropriate length at critical period[21]. Both negative and positive memories can be reflected in brain cortex, and its simulations fits very well with experiments in the relationship of human intelligence and cortical thickness, individual differences in brain[22]. The PNN also considered the memory engram cells that strengthened synaptic strength[23]. And paper found that 1064-nm Transcranial photobiomodulation (tPBM) applied to the right prefrontal cortex (PFC) improves visual working memory capacity [24], the effect of PNN memory structure may be the same with smaller losses in signals.

We can regard PNN as a special Recurrent Neural Network (RNN), each input variable corresponds to neurons shared connection weights over a period of time interval; the weights are updated by the MSE loss of the activation function of output within this synaptic effective range. The synaptic effective range is reflected in the time interval, for which the real value of the simulation would lead to gradient-based change in the synaptic effective range by Back Propagation. The Back Propagation of PNN includes shared connection weights and synaptic effective range weights. A simulation of PNN was conducted on the cognitive processes in the brain from infancy to senile phase, which is interpreted by the observation of decreasing the synapse population and increasing the minimum of synaptic effective range in PNN evolution of synapse formation, hence the loss of diversity and plasticity. This explanation is similar to the Dr. Luo and his colleagues’ research, and on PNN which shows that the synapse formation in a certain extent may inhibit dendrite. And we also analyzed the different brain plasticity by Tables at critical or the closure of critical period. When ORPNN contains both astrocytic synapse formation

cortex memory persistence factor and astrocytes phagocytose synapses factor will have better results in correlation coefficients of Tables respectively at critical period.

The cosine filter is used in the tests for comparing the result of the three cases, namely gradient optimized synaptic effective range (ORPNN), random synaptic effective range (RRPNN), and constant synaptic effective range (CRPNN). The result indicates that the ORPNN runs the best. Through the PNN tests, we found that the astrocytic cortex memory persistence factor, like the astrocytes phagocytose synapses factor, produces the effect of reducing the local accumulation of synapses. Considering both negative and positive cortex memories persistence yields better results than considering only positive cortex memory persistence. In the calculation to update the synaptic effective range, the PNN in which only the effect of astrocytes phagocytose synapses is considered regardless of the gradient update, proves simple and effective. Therefore, is it possible to reduce the number of animal experiments and their suffering by simulating and planning the factors of biological experiments through Deep learning?

1 Introduction

Researchers in the Deep Learning community have long regarded simulation of the human brain as an important means of advancing Neural Networks (NN). In machine learning and computational neuroscience, Artificial Neural Networks (ANN) are used as mathematical and computational models that mimic the structure and function of biological Neural Networks. Estimations and approximations conducted by the functions have witnessed great success over the recent decades. The more commonly used Neural Networks models today include Perceptron in 1957 [1], Hopfield network in 1982 [2], Boltzmann in 1983 [3], Back Propagation (BP) in 1986 [4], Convolutional Neural Networks (CNN) in 1989 (from Neocognitron [5] to CNN [6]), Spiking Neural Networks (SNN) in 1997 [7], Long Short-Term Memory (LSTM) in 1997 [8], Deep Belief Network (DBN) in 2006 [9], Deep Neural Networks (DNN) in 2012 [10], Deep Forest (DF) in 2019 [11] and Deep Residual Learning (ResNet) in 2016 [12].

Human brains can be very flexible due to their plasticity. Neural activity can induce the strengthening or weakening (potentiation or depression) of synapses to produce plasticity. The brain plasticity therefore refers to the connections of synapses and neurons, and to establish new connections as a result of learning and experiencing, thus exerting impacts on the behaviors of individuals. The synapses are the roles between neurons permitting the transmission of signals or stimulus. Therefore, our new NN model takes into account not only the synaptic connections, but also how the synaptic effective range at current and history moments changes plastically with the iteration, particularly at critical period, namely, in addition to the shared weights of the current and memory synaptic connections, it also considers the weights of the

current and memory synaptic effective ranges (brain plasticity) and gradient information (synapse formation) at critical period.

Last year, researchers presented the *One Hundred Year Study on Artificial Intelligence (AI100) 2021 Study Panel Report*, in which one question concerns how much progress we have made in UNDERSTANDING the PRINCIPLES of HUMAN INTELLIGENCE. First, a basic tenet of cognitive neuroscience is that individual characteristics such as working memory and executive control are critical for domain-independent intelligence, which determines an individual’s performance on all cognitive tasks regardless of mode or subject. A second hypothesis gaining traction is that higher-ability persons enjoy more efficient patterns of brain connectivity—higher-level brain regions in the parietal-frontal cortex. The third concept is more revolutionary, which suggests that the neural correlates of intelligence are dispersed throughout the brain. According to this theory, human intelligence is fundamentally flexible, constantly updating past information and making new predictions [13]. The new NN proposed in this thesis is grounded on the first and third notion, taking into consideration the current and past brain plasticity and current gradient informational and memory positive and negative gradient informational synapse formation at critical period and closure of critical period.

Scientists of MIT’s Picower Institute have unveiled for the first time how this balance is achieved in synapses: Professor Mriganka Sur likens this behavior to a massive school of fish in the sea. Immediately when the lead fish changes direction, other fish will follow suit, presenting a delicate marine “dance”. “Collective behaviors of complex systems always have simple rules. When one synapse goes up, within 50 micrometers there is a decrease in the strength of other synapses using a well-defined molecular mechanism.” the scientists stated [14]. The lead behavior of the school of fish is well embodied in our PNN. However, our Neural Network is no longer confined to the simple physical concept of synaptic strength rebalance - it treats synapses as a group of intelligent agents to achieve synaptic strength rebalance.

Findings largely consistent with that of Dr. Luo’s team at Stanford University in PNN tests are obtained in our study, that is, the synapse formation will inhibit dendrites generation to a certain extent [15], with the reason shown in our simulation results being that synaptic growth leads to a reduction in changes in synaptic effective range, which disrupts diversity and plasticity of brain.

The Alcino J Silva’s team suggested that memory ensembles recruit presynaptic neurons during learning by a retrograde mechanism [16]. The retrograde mechanism reflected in memory retrieval process of PNN.

The Alvarez-Buylla’s lab proposed that recruitment of young neurons to the primate hippocampus decreases rapidly during the first years of life, and that neurogenesis in the dentate gyrus does not continue, or is greatly rare, in adult humans [17]. The PNN gave the simulation results of decrease of neurons because of synapse formation.

But Boldrini et al suggested healthy older subjects display preserved neurogenesis. It is possible that ongoing hippocampal neurogenesis sustains human-specific cognitive function throughout life [18]. And PNN's guess decline in neurogenesis may be repaired by a new and longer circuit in late iteration.

The finding has significant implications for the learning and further development of NN. Moreover, the mechanism of our NN is basically consistent with that of the latest brain plasticity study conducted by MIT, in which researchers found that as a synapse strengthens, neighboring synapses automatically weaken themselves to compensate [14]. In tests, possible explanations of dendrite morphogenesis are derived, which demonstrate that dendrite generation, to a certain extent, is curbed by synapse formation [15]. Unconventional astrocyte connexin signaling hinders expression of extracellular matrix-degrading enzyme matrix metalloproteinase 9 (MMP9) through RhoA-guanosine triphosphatase activation for controlling critical period closure. The effect of astrocyte impacts on brain plasticity and synapse formation is an important mechanism of our Neural Network at critical period, and failures by the closure of critical period result in neurodevelopmental disorders [19]. In the model at critical period, the hypothesis is the best previous brain plasticity affects current brain plasticity and the best previous synapse formation, relatively good and relatively inferior synapse formation affects current synapse formation. While their experimental research features a combination of cutting-edge imaging and genetic tools, our study lays more emphasis on the model, derivation and simulation of a new NN. At the same time, the current and memory brain plasticity-the synaptic effective range are taken into consideration. Furthermore, the architecture of new NN is based on current gradient informational and memory positive and negative gradient informational synapse formation for cortex memory persistence. By simulations, the PNN gave the two cases with and without negative cortex memories persistence. And the paper proposed $\alpha 7$ -nAChR-dependent astrocytic responsiveness is an integral part of the cellular substrate underlying memory persistence by impairing fear memory[20]. In addition, memory brain plasticity involves the plus or minus disturbance- astrocytes phagocytose synapses factor, through which the dynamic synaptic strength balance is achieved [21]. The effect of astrocyte made local synaptic effective range remain in an appropriate length at critical period [21]. Our new NN may give more inspirations to experiments in the relationship of human intelligence and cortical thickness, individual differences in brain [22]. By using learning-dependent cell labeling, Dr. Susumu Tona-gawa and his team identified an increase of synaptic strength and dendritic spine density specifically in consolidated memory engram cells. For improving synaptic strength in PNN, the memory retrieval process by memory engram cells includes memory negative and positive gradient information, and memory engram cells are helpful to the memory retrieval process [23]. In this study, researchers found that 1064-nm tPBM applied to the right prefrontal cortex (PFC) improves visual working memory capacity [24], and PNN has same

effect for improving memory capacity by memory structure. The Dr. Christian Kerskens and David López Pérez of Trinity College Institute of Neuroscience’s findings suggest that they may have witnessed entanglement mediated by consciousness-related brain functions, because consciousness-related or electrophysiological signals are unknown in nuclear magnetic resonance (NMR). Those brain functions must then operate non-classically, which would mean that consciousness is non-classical [25], so PNN introduces brain plasticity of extracted relatively good or inferior memories brains plasticity, which reflected consciousness by quantum computing. Priya Rajasethupathy research group of Rockefeller University developed longitudinal simultaneous imaging in hippocampus, thalamus, and cortex of mouse brain, and propose a thalamo-cortical circuit that gates memory consolidation, and suggest a mechanism suitable for the selection and stabilization of hippocampal memories into longer-term cortical storage [26]. In simulations of PNN, it converts hippocampal non-classical exacted memories to long-term classical memories, maximum of directional derivatives is gradient, and barriers will lead to exponential decay of wave function.

Researchers from the University of Oxford, Pompeu Fabra and Indiana University published an article in Communications Physics, and used magnetoencephalography (MEG) technology to analyze turbulence throughout the brain, and the study found that efficient information transmission of the brain relies on turbulence, through which the phenomenon of turbulence in rapid neuronal brain dynamics can be directly measured [27].

Paper’s work suggests a model in which impaired MCH-dependent synaptic function in CA1 and perturbed REM sleep synergistically compromise neuronal homeostasis, contributing to aberrant neuronal activity in CA1[28]. It is also indirectly proved our possible mechanism of Alzheimer’s disease

Our newly proposed NN is named the Plasticity Neural Network (PNN). Synaptic competition causes the enhancement of signal-stimulated synapses to be reflected in an increase in synaptic effective range, while the weakening of peripherally stimulated synapses is reflected in a shortening of synaptic effective range.

The following papers are academic frontiers in neuroscience and artificial neural networks which we endeavor to make connections with our PNN.

Based on the mechanism of flow stability, professor Hua-Shu Dou proposed energy gradient theory. The maximum of directional derivatives might be modified by a critical angel, and the angle 0 turns to α_c [29].

Their research shows that SynCAM 1 actively limits cortical plasticity in the mature brain. Plasticity tapers off when the brain matures and the conclusion is sufficiently substantiated by visual input in adult animal models [30]. As was stated by Dr. Biederer of Tufts University’s medical School, “Our research has identified a mechanism underlying the control of brain plasticity, and most excitingly, we can demonstrate that there is an active process of inhibiting plasticity in the adult brain.”

The Self-Back Propagation (SBP) phenomenon, first discovered in hippocampal neurons [31, 35], involves cross-layer Back Propagation (BP) of Long-Term Potentiation (LTP) and Long-Term Depression (LTD) from output to input synapses of a neuron to enable the strengthening or weakening of synaptic connections. Other forms of nonlocal spreads of LTP and LTD in the pre- and post-synaptic neurons have already been researched extensively [31, 32, 35]. The SBP phenomenon induces a form of nonlocal activity-dependent synaptic plasticity that may endow developing neural circuits with the capacity to modify the weights of input synapses on a neuron in accordance with the status of its output synapses [32]. The existence of SBP was demonstrated in developing retinotectal circuits in vivo [33, 34]. These papers endeavor to shed light on plasticity rules involving activity-dependent modification of synapses to obtain synaptic activity [31–35].

Bertens and Lee proposed an evolvable neural unit (ENU) that can evolve individual somatic and synaptic compartment models of neurons in a scalable manner and try to solve a T-maze environment task [36].

Wang and Sun stated that in a unidirectional RNN, the linking with the emotion regions and the somatic motor cortex includes three basic units: input units arriving from the emotion regions, only one hidden unit composed of self-feedback connected medial prefrontal cortex neurons, and output units located at the somatic motor cortex [37]. If they used PNN regardless of RNN may give more insights in their research.

In the simulations of PNN in brain plasticity at critical period, we had an idea to modify the synapses for repairing brain plasticity, and later we found this paper to build and remodel of synapses [38].

Instead of conducting research simply on the basis of Self-Back Propagation phenomenon, the PNN we propose in this thesis focuses more on plasticity and strength rebalance as a result of its tapering off -the brain from infancy to senile phase during critical period and the closure of critical period. The model also delves into the competition of brain plasticity which introduces a novel form of current gradient informational and memory positive and negative gradient informational synapse formation, as well as current and memory brain plasticity at critical period. The strengthening and weakening of synaptic connections help to curb and boost current and history synaptic effective ranges, resulting in an increased accuracy of PNN.

The research, based on Genetic Algorithm or Particle Swarm Optimization in search of the connection weights for each time interval of the dynamic problems, and on PNN to find the weights of the connection and the effective range, takes into account the specificity of the new coronavirus variant, whose viral strain is highly variable. The viral load of the Delta (or Omicron) strain is 1,260 times higher than the prevalent strain of last year, thus doubling the infectious rate of last year's original strain. The major difference between PNN and RNN is that the former has a formula to estimate the parameters (shared connection weights) for their respective parameters' ranges (synaptic effective range weights) at critical period. So PNN is based on the practical

dynamic problem in an effort to obtain the new NN. As for the selection of the appropriate mechanism, we chose the hypotheses and possible explanations of synaptic strength rebalance, competition and effect of astrocyte [14–27]. In this way, not only the architecture of NN is transformed by current gradient information, but also memory positive and negative gradient informational synapse formation and memory brain plasticity are taken into account. The memory gradient information needs to consider astrocytic synapse formation cortex memory persistence factor (including both negative and positive memories). By simulations, the PNN gave the two cases with and without negative cortex memories persistence. And the paper proposed $\alpha 7$ -nAChR-dependent astrocytic responsiveness is an integral part of the cellular substrate underlying memory persistence by impairing fear memory [20]. In addition, memory brain plasticity involves the astrocytes phagocytose synapses factor [21]. And also comparing with the simulations and experiments in the relationship of human intelligence and cortical thickness, individual differences in brain [22]. In PNN, the memory retrieval process includes memory negative and positive gradient information, and used in formula (2) [23]. And PNN has same effect for improving memory capacity by memory structure of salient point and concave point [24].

After representing the synaptic plasticity competition in Formula (2), strength rebalance in Formula (3), current gradient informational and memory positive and negative gradient informational synapse formation at critical period in Formula (2), current and memory brain plasticity at critical period in Formula (4), cosine filter is used in tests to verify the PNN and compare the results of the following three situations: the case dubbed as CRPNN, in which the synaptic effective range for various neurons remains unchanged; the RRPNN case, in which synaptic effective range for each neuron generates in a random manner; the last one is the ORPNN case, in which optimization of synaptic effective range connects neurons with iterations. The findings also show that synapse formation will, to some extent, inhabit the tests of PNN. And we also analyzed the different brain plasticity by Tables at critical period or the closure of critical period. The effect of astrocytic synapse formation memory cortex persistence factor and astrocytes phagocytose synapses factor in Tables.

2 Method

We developed PNN under the premise that the sum of synaptic effective ranges of these neurons’ connections remains a constant value for the synaptic strength rebalance. For RNN, the size of training sets has been determined by sum of synaptic effective ranges l_{\max} . This hypothesis works for RNN as well as BP. However, synapse formation will lead to convergence and the loss of plasticity, therefore diminishing the cognitive abilities of PNN. For RNN, the input variables correspond to the different types of neurons’ within a time interval, and each time interval corresponds to a connection weight. And the

weight is updated by the MSE loss of the activation function of output within this synaptic effective range. The synaptic effective range is reflected in the time interval, and alters with the gradient by simulating real value- training sets with iterations.

Formula (1) and (2) are both obtained through the reasoning of MSE loss function gradient. The activation function for the amount of change in the output result is processed through the tanh function.

Formula (1) updates the shared connection weight of the k th synapse of the m th input neuron, $f()$ represents the output of different variables and synapses, m represents the label of the input variable, k represents label of synapses connecting two neurons, and the range of values of time interval t is $[n3(m, k) \ n3(m, k+1)]$. $h(t)$ indicates actual output, and $f(t)$ represents desired output. $n3(m, k)$ and $n3(m, k+1)$ depict the location of the m th input variable and k th synaptic initiation and termination points. $\eta = 1/1E3 \times (j_{\max} - j)/j_{\max}$, namely, the learning rate is reflected in formulas (1) and (2).

$$g_w(m, k) = [f(t) - h(t)] \times \Delta f(t-1)'_{w(m,k)}/1E3 \quad (1)$$

$$\times (j_{\max} - j)/j_{\max} \times [1 - \Delta f(t-1)^2]$$

$$w(m, k) = w(m, k) - g_w(m, k)$$

The synaptic effective range weights of the m th input variable and the k th synapse is updated by Formula (2). The relationship between the synaptic location and the effective range satisfies the equation $n3(m, k+1) - n3(m, k) = n_1(m, k)$, in which $n_1(m, k)$ represents the synaptic effective range. When the synaptic position of the lead neurons is changed, these neurons, much like the heads in a massive school of fish, also exerts an impact on the postsynaptic neurons. Formula (2) considers current gradient informational and memory positive and negative gradient informational synapse formation updated by the gradient of the best previous synaptic effective range weight $g_r(m, k)_{best}$, or gradient of relatively inferior synaptic effective range weight $g_r(m, k)_{worse}$ or relatively good synaptic effective range weight $g_r(m, k)_{better}$, so that architecture of PNN bears current and memory gradient information at critical period. With reference to Formula (3), Formula (2) $n(m, k)'_{r(m,k)} = [\frac{-r(m,k)}{\text{sum}(r(m, :))^2} + \frac{1}{\text{sum}(r(m, :))}] \times (l_{\max} - k_{\max} \times l_{\min})$. $MW_{i,i=1,2,3}$ is memory weight.

$$g_r(m, k) = [f(t) - h(t)] \times \Delta f(t-1)'_{n1(m,k)} \times n_1(m, k)'_{r(m,k)}$$

$$\times \eta \times [1 - \Delta f(t-1)^2] = [f(t) - h(t)]$$

$$\times \Delta f(t-1)'_{n1(m,k)}/1E3 \times (j_{\max} - j)/j_{\max} \times [1 - \Delta f(t-1)^2] \quad (2)$$

$$\times [\frac{-r(m, k)}{\text{sum}(r(m, :))^2} + \frac{1}{\text{sum}(r(m, :))}] \times (l_{\max} - k_{\max} l_{\min})$$

$$r(m, k) = r(m, k) - g_r(m, k)$$

$$\text{or } r(m, k) = r(m, k) - g_r(m, k) + [g_r(m, k)_{best} - g_r(m, k)] \times M$$

$$\begin{aligned} \text{or } r(m, k) &= r(m, k) - g_r(m, k) \\ &+ [MW_1 \times g_r(m, k)_{best} + MW_2 \times g_r(m, k)_{worse} - g_r(m, k)] \times M \\ MW_1 &= 0.6666, MW_2 = 0.3333 \end{aligned}$$

$$\begin{aligned} \text{or } r(m, k) &= r(m, k) - g_r(m, k) \\ &+ [MW_1 \times g_r(m, k)_{best} + MW_2 \times g_r(m, k)_{worse} \\ &+ MW_3 \times g_r(m, k)_{better} - g_r(m, k)] \times M \\ MW_1 &= 0.5, MW_2 = 0.25, MW_3 = 0.25 \end{aligned}$$

Formula (3) serves to update the range of connecting neurons at the k th synapse of the m th input variable, and normalization of result is achieved through $r(m, k)/\text{sum}(r(m, :))$ in Formula (3). The result of $r(m, k) = r(m, k) - g_r(m, k) + [0.6666 \times g_r(m, k)_{best} + 0.3333 \times g_r(m, k)_{worse} - g_r(m, k)] \times M$ may be better than $r(m, k) = r(m, k) - g_r(m, k)$ in simulation, because negative and positive memories reflecting the diversity. If Formula (2) just has current gradient information, $r(m, k) = r(m, k) - g_r(m, k)$, else if Formula (2) includes current and memory gradient information, $r(m, k) = r(m, k) - g_r(m, k) + [0.6666 \times g_r(m, k)_{best} + 0.3333 \times g_r(m, k)_{worse} - g_r(m, k)] \times M$ needs to consider forgotten memory in synapse formation, cortex memory persistence of astrocytic function gradually lost by aging. The gradient method to update the synaptic effective range weights by long-term memory means $g_r(m, k)_{best}$ or $g_r(m, k)_{worse}$. Strong working memory or short-term memory was consolidated and became long-term memory. Short-term memory brain plasticity goes through brain from hippocampus to cortices by directional derivative. The strong working memory brain plasticity turns to long-term memory means maximum of directional derivatives, and maximum of directional derivatives is gradient.

The derivation of cortex memory persistence factor is as follows, may happen in memory engram cells of different cortices: The update of $r(m, k) = r(m, k) - g_r(m, k)$ is based on the gradient descent method. From $r(m, k) = r(m, k) - g_r(m, k)_{best}$, we can obtain $r(m, k)_{t+1} = r(m, k)_t - g_r(m, k)_{best}$, $r(m, k)_{t+1}$ is the best previous synaptic effective range weight, and $g_r(m, k)_{best}$ is the gradient of the best previous synaptic effective range weight. Time reversal from $t + 1$ to t to return to in situ to maintain memory can also be written as $r(m, k)_t = r(m, k)_{t+1} + g_r(m, k)_{best}$, after which, by adding $r(m, k)_{t+1} = r(m, k)_t - g_r(m, k)$ and $r(m, k)_t = r(m, k)_{t+1} + g_r(m, k)_{best}$, we

get $r(m, k) = r(m, k) - 0.5 \times g_r(m, k) + 0.5 \times g_r(m, k)_{best}$. Considering the flexibility of learning rate, it can also be written as $r(m, k) = r(m, k) - g_r(m, k) + [g_r(m, k)_{best} - g_r(m, k)] \times M$. If we take both positive and negative memories into account, introducing the gradient of the best previous synaptic effective range weight $g_r(m, k)_{best}$, gradient of relatively inferior synaptic effective range weight $g_r(m, k)_{worse}$ and gradient of relatively good synaptic effective range weight $g_r(m, k)_{better}$, therefore the equation can be modified as follows: $r(m, k) = r(m, k) - g_r(m, k) + [0.6666 \times g_r(m, k)_{best} + 0.3333 \times g_r(m, k)_{worse} - g_r(m, k)] \times M$ or $r(m, k) = r(m, k) - g_r(m, k) + [0.5 \times g_r(m, k)_{best} + 0.25 \times g_r(m, k)_{worse} + 0.25 \times g_r(m, k)_{better} - g_r(m, k)] \times M$. As indicated in Fig.1, the best previous solution appears at time point $j+1$, with the smallest Loss. And the next generation demonstrates an upward trend, featuring a relatively inferior solution with an increase in Loss which appears at time point $j+3$. The generation demonstrates a downward trend, featuring a relatively good solution with a decrease in Loss which appears at time point $j+5$. The relatively good and inferior gradient information in synapse formation of retrograde circuit like the folds of the brain.

In derivation of formula (2), the $[MW_1 \times g_r(m, k)_{best} + MW_2 \times g_r(m, k)_{worse} + MW_3 \times g_r(m, k)_{better} - g_r(m, k)]$ of $r(m, k) = r(m, k) - g_r(m, k) + [MW_1 \times g_r(m, k)_{best} + MW_2 \times g_r(m, k)_{worse} + MW_3 \times g_r(m, k)_{better} - g_r(m, k)] \times M$ illustrated that recruitment of presynaptic neurons is triggered by downstream neurons through a retrograde mechanism[16], so the memory gradients $MW_1 \times g_r(m, k)_{best}$, $MW_2 \times g_r(m, k)_{worse}$, $MW_3 \times g_r(m, k)_{better}$ are positive, and the current gradient $-g_r(m, k)$ is negative.

We hypothesize that the hippocampus stores memory brain architecture as r , this r may be affected by quantum entanglement from the heart frequency and the brain architecture. If r is transmitted from the hippocampus to the first cortex of the brain, memory produces a rate of change $\frac{\partial r}{\partial n_1}$, and the second cortex conducts memory through the rate of change to take $\frac{\partial^2 r}{\partial n_1 \partial n_2}$, and the rate of change of this cortex continues to conduct to achieve the flow of memory, ignoring the difference between different cortices, then the n th cortex is the n th derivative $\frac{\partial^n r}{\partial n_1^n}$ of brain plasticity. This is a bit like chain-derivation in Deep learning, Deep learning from input to output, that is, from the n th cortex on the outside to the hippocampus on the inside. The turbulent movement of the mnemonic logarithmic spiral spreading from one cortex to another is only a loss of energy, but the memory engrams are still approximate.

Turbulence occurs from the hippocampus to the first cortex, memory may be a first-order derivative of brain plasticity, means gradient or Jacobian matrix. Turbulence occurs from the first cortex to the second cortex, memory may be the first derivative of the brain plasticity Jacobian matrix, that is, second derivative of the brain plasticity, the Heisen matrix. $h_r(m, k)$ stands for the Heisen matrix. At this time, the gradient method that updates synaptic effective range is changed into Newton's method. Formula (2) can be further modified to take into account the case of the Heisen matrix. Alzheimer's disease may first be positive about in the $g_r(m, k)$ of the first cortex, followed

by positive gradient in the $\frac{g_r(m,k)}{h_r(m,k)}$ of the second cortex, and positive and negative changes in these derivatives lead to disturbances in synaptic excitation and inhibition. It is shown in Fig. 1(h). Similarly, memory flows to the n th external cortex may be the n th derivative of brain plasticity. We suspect that curly hair indicates that the brain has strong energy, and energy can be transmitted from the hippocampus to the epidermis of the brain at a critical angle of the cortex, so people with curly hair are not prone to Alzheimer's disease.

Backpropagation from the hippocampus to different cortexes, it requires higher-order optimization to process simple signals, indicates that the external part of the brain needs higher-order optimization, it is also possible to reduce the complexity of the calculation. Forward propagation from different cortexes to the hippocampus, complex signals require more fear memories to jump out of the local optimal solution, that is, more fear memories are needed inside the brain.

If we take the logarithmic spiral of the partial mnemonic brain architecture $r_m(m, k) = ae^{b\theta}$, that is, the memory may be two-dimensional logarithmic spiral in a certain cortex, only having the angular strain θ , and the second cortex mnemonic architecture is $\frac{dr_m(m,k)}{d\theta} = abe^{b\theta}$, because turbulence diffuses the n th cortex mnemonic architecture $\frac{d^{n-1}r_m(m,k)}{d\theta^{n-1}} = ab^{n-1}e^{b\theta}$, and take $b < 1$ means that the memory gradually weakens transmission to the upstream brain regions, the logarithmic spiral $n - 1$ th derivative is the memory engram shapes are approximate, but the image quality of the memory engram is compressed, a is related to the synaptic effective range weight, b is related to the synaptic connection and effective range weights. The mnemonic architecture of the downstream first cortex is r_m , and the mnemonic architecture of the upstream n th cortex may be approximately the $n - 1$ th derivative of r_m .

The formula for memory engram is given and the $n - 1$ th derivative of r_m . The following situations are met:

- 1 The memory engram flows by turbulence from the downstream brain regions to the upstream brain regions, and the shape of the memory engram remains unchanged, because the resistance along the way and the pipe diameter gradually decreases, and the image quality of the memory engram will be compressed because of the derivation of memory engram.
- 2 The memory engram moves from the upstream brain regions to the downstream brain regions, and the shape of the memory engram remains unchanged, but there is no the resistance along the way and the pipe diameter gradually increases, and the memory engram image quality will not be compressed.
- 3 If the large middle blood vessels and large middle aqueducts in the downstream brain regions are destroyed, the analysis of reverse turbulence makes reversal of the situation 1 and 2. Situation 1: Memory engram does not lose image quality, and it will be better to obtain memory engram, but hallucinations may occur due to downstream information redundancy; Situation 2:

Turbulence occurs across the cortex and memory engram loses image quality from upstream to downstream.

- 4 Our memory engram may be a two-dimensional logarithmic spiral in the brain cortex, which is derived from only one angle strain variable for turbulent movement across brain regions.

The angle ψ between the logarithmic spiral tangent and the radius, which can be calculated that, $\psi = \tan^{-1} \frac{r_m(m,k)}{\frac{dr_m(m,k)}{d\theta_1}} = \cot^{-1} \frac{\frac{dr_m(m,k)}{d\theta_1}}{r_m(m,k)} = \cot^{-1} b$, if b is too small, $\cot^{-1} b = \frac{\pi}{2}$, the logarithmic spiral is close to the circle, and the smooth surface weakens the synaptic connection ability. The critical angle of turbulence α can be understood in this way, only considering the angular motion of the logarithmic spiral, tangential strain of logarithmic spiral along the spiral $\theta_1 = \frac{\pi}{2} - \psi$ and tangential strain of logarithmic spiral angular motion θ_2 . When they become the force and counter-force, $\theta_1 + \theta_2 = 0$, which can be calculated that, $\alpha = -\tan^{-1} b = \tan^{-1} \frac{\frac{dr_m(m,k)}{d\theta_2}}{r_m(m,k)} = \theta_2$. θ_2 should be at least greater than the action of θ_1 , which can be turned to turbulence, and the nonlinear movement of the logarithmic spiral means the strain of the brain, which from the hippocampus to the prefrontal lobe, that is, the strain of the brain and the strain of memory may be an equal and opposite reaction, the angle changes in space-time are $\tan^{-1} b$, so the geometry of the longitudinal section of the brain is like a spiral, with the beginning or O point of the spiral is the prefrontal lobe and ending in the hippocampus. If you do not consider different brain regions, only suppose the mechanical property of the isotropy of the brain, then the brain longitudinal section is more like the spiral. And the value of the critical angle is related to the mnemonic connection weight, and the life span of the logarithmic spiral is related to the mnemonic effective range and connection weights. See Fig. 1(i) and 1(j).

$\theta_1 = \tan^{-1} b$ critical angle increase hinders the transmission of information between brain regions. The synapse formation increases the synaptic effective range weight associated with a , it has nothing to do with the critical angle, which increases the life span of the logarithmic spiral. And the loss of immune cells because of the reverse turbulence, which leads to neuroinflammation and increases the shared connection and effective range weights associated with b , which in turn increases the critical angle. Both the enlargement of a and b may impair cognition.

The element $g_r(m, k)_{worst, i}$ or $g_r(m, k)_{better, i}$ of history set $WORSE = \{g_r(m, k)_{worst, i} \in N^*\}$ or $BETTER = \{g_r(m, k)_{better, i} \in N^*\}$ also can be considered in the formula (2), and latest $g_r(m, k)_{worst}$ or $g_r(m, k)_{better}$ could be replaced by later $g_r(m, k)_{worse, i}$ or $g_r(m, k)_{better, i}$. The gradient information of later element $g_r(m, k)_{worse, i}$ or $g_r(m, k)_{better, i}$ is stored in memory engram cells of cortexes, namely larger i of $g_r(m, k)_{worst, i}$ or $g_r(m, k)_{better, i}$ will be selected with upper probabilities.

Why formula (2) chooses the elements of history set $WORSE$ or $BETTER$?

Based on optimality principle, the relatively good gradient information can help to search optimal solution, and the relatively inferior gradient information can help to improve diversity of searching optimal solution. The location of relatively inferior gradient information is salient point, the directions of search both are downward and become more efficient. The location of relatively good gradient information is concave point, the directions of search both are upward and improve the efficiency.

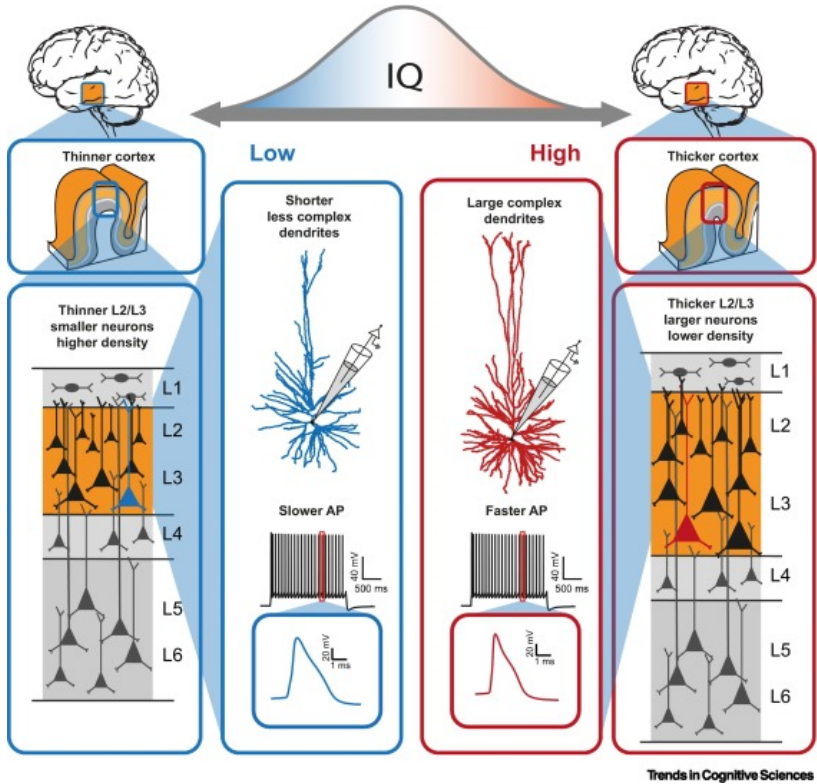
But memory-forgotten means that the signals from input to output units dissipate with resistances in brain and do not activate the relevant gradient information, and these resistances in brain increase by aging.

In the model at critical period, the hypothesis is the best previous synapse formation and relatively inferior synapse formation affects current synapse formation. Bad memory of synapse formation $M = \exp(-7 \times j/j_{\max}) \times rand$ or good memory $M = \exp(-5 \times j/j_{\max}) \times rand$ can be called the astrocytic synapse formation cortex memory persistence factor. j/j_{\max} illustrates the decreasing weights of factor we present at critical period in M .

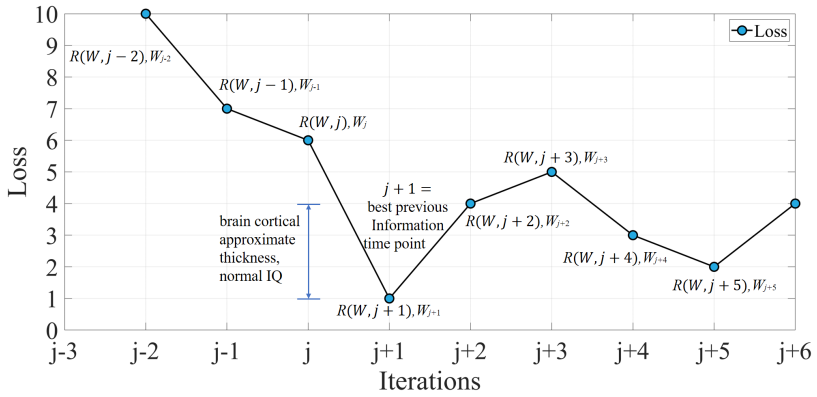
$$n_1(m, k) = \frac{r(m, k)}{\text{sum}(r(m, :))} \times (l_{\max} - k_{\max}l_{\min}) + l_{\min} \quad (3)$$

For a certain input variable, the neuron has a total of k_{\max} synapses, l_{\min} shows that the synaptic range change enjoys a certain degree of plasticity, and the minimum synaptic effective range is l_{\min} . $g_r(m, k)$ controls l_{\min} with iterations and represents the elasticity or plasticity of synapses, and if the value of l_{\min} is overly small, the change of $n_1(m, k)$ will be too elastic and may make the test results deteriorate. k_{\max} indicates the synapse population involved in the neurons from input to output units, and l_{\max} represents the sum of ranges of time series and is a constant. For the signal of a neuron (i.e., an input variable), when one synapse strengthens, there must be surrounding synapses that are weakened. In the case when $l_{\max} = k_{\max} \times l_{\min}$, i.e., the case in which the synaptic effective range is constant, the $n_1(m, k) = l_{\min}$ is also a constant value. That is, for $l_{\min} = l_{\max}/k_{\max}$, constant-range synapses also satisfy Formula (2) and Formula (3). Formula (2) can be named the synaptic competitive formula, and Formula (3) can be dubbed as the synaptic strength rebalance formula.

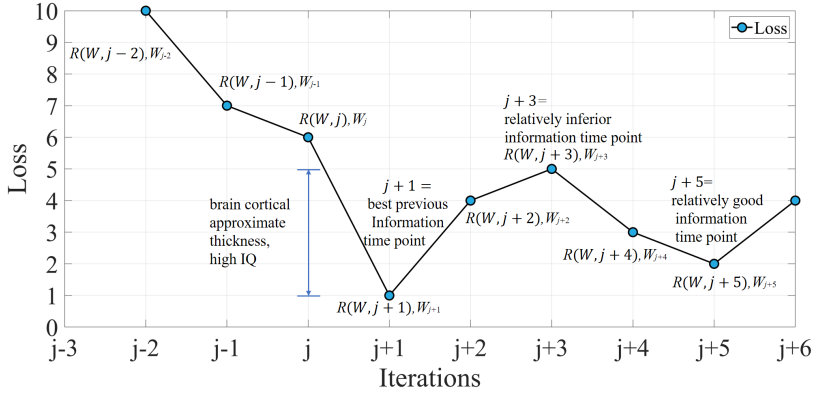
$$\begin{aligned}
r(m, k) &= r(m, k) - [r(m, k)_{best} - r(m, k)] \times rand + P \\
\text{or } r(m, k) &= r(m, k) \\
&+ [MW_1 \times r(m, k)_{best} + MW_2 \times r(m, k)_{worse} \\
&+ MW_3 \times r(m, k)_{better} - r(m, k)] \times rand + P \\
MW_1 &= 0.5, MW_2 = 0.25, MW_3 = 0.25 \\
\text{or } R &= r(m, k)_{best} + rand \times [r(m, k)_{best} - r(m, k)_{better}] \\
r(m, k)_{temp, better} &= \text{sign}(rand - 0.5) \times \beta \times \\
&|r(m, k)_{best} + rand \times [r(m, k)_{best} - r(m, k)_{better}] \\
&- \sum_{i=j-LEN+1}^j \frac{r(m, k)_{i, better}}{LEN} | \times \ln\left(\frac{1}{rand}\right) \\
r(m, k)_{temp, worse} &= \text{sign}(rand - 0.5) \times \beta \times \\
&|r(m, k)_{best} + rand \times [r(m, k)_{best} - r(m, k)_{better}] \\
&- \sum_{i=j-LEN+1}^j \frac{r(m, k)_{i, worse}}{LEN} | \times \ln\left(\frac{1}{rand}\right) \\
Q_P &= (rand > 0.5) \times r(m, k)_{temp, better} \\
Q_N &= (rand > 0.5) \times r(m, k)_{temp, worse} \\
P &= \text{sign}(rand - 0.5) \times rand \times (j_{max} - j) / j_{max} \\
r(m, k) &= r(m, k) + rand \times [MW_1 \times R + MW_2 \times Q_N + MW_3 \times Q_P - r(m, k)] + P \\
MW_1 &= 0.5, MW_2 = 0.25, MW_3 = 0.25
\end{aligned}$$



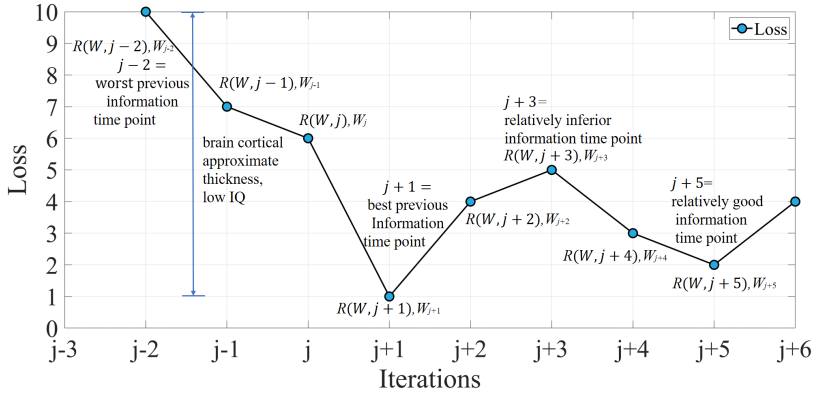
(a)



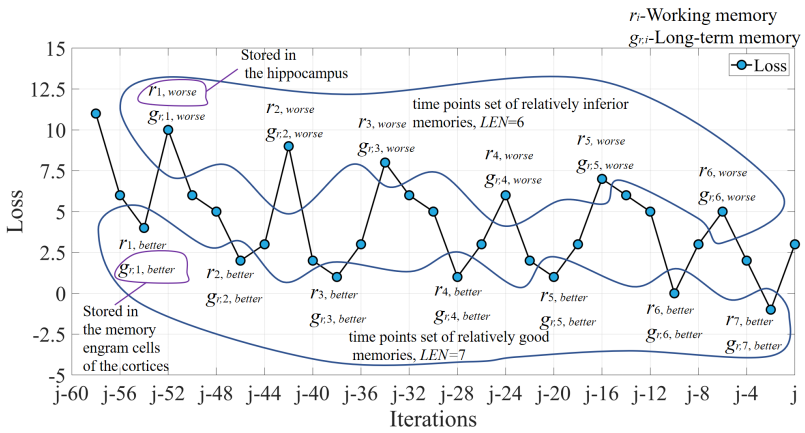
(b)



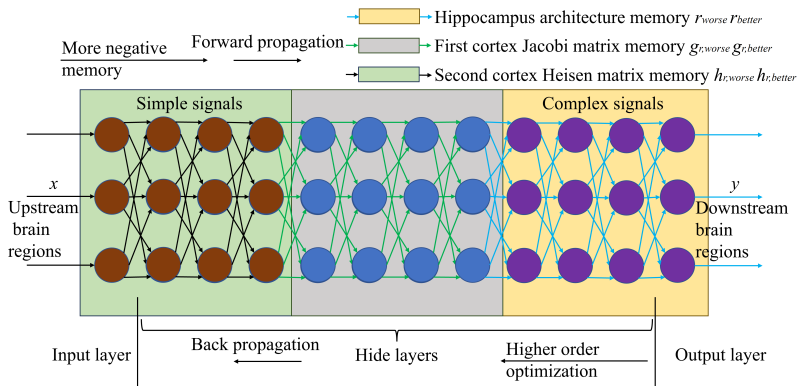
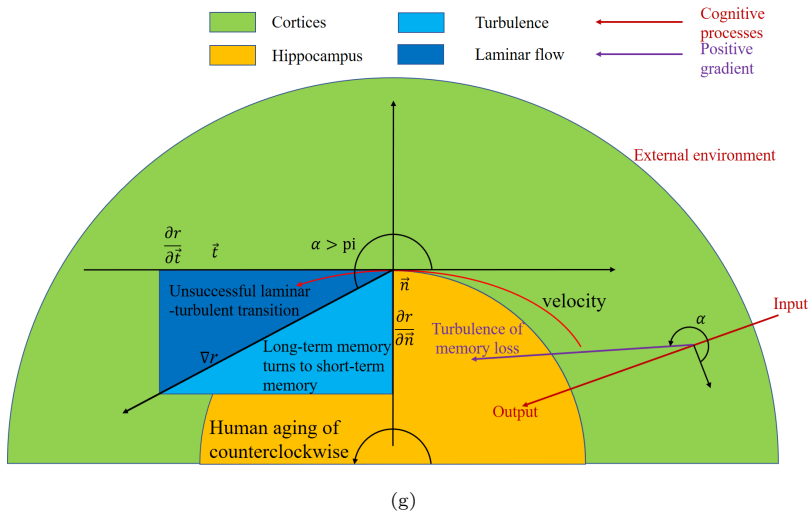
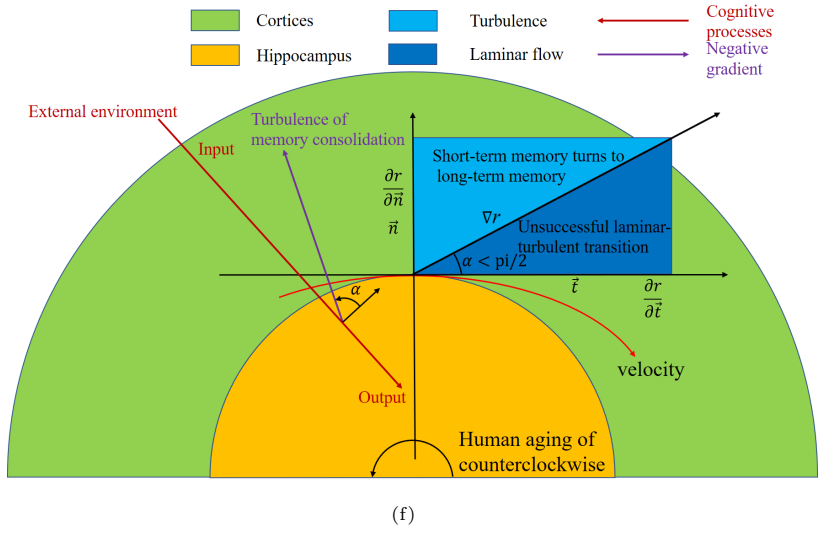
(c)

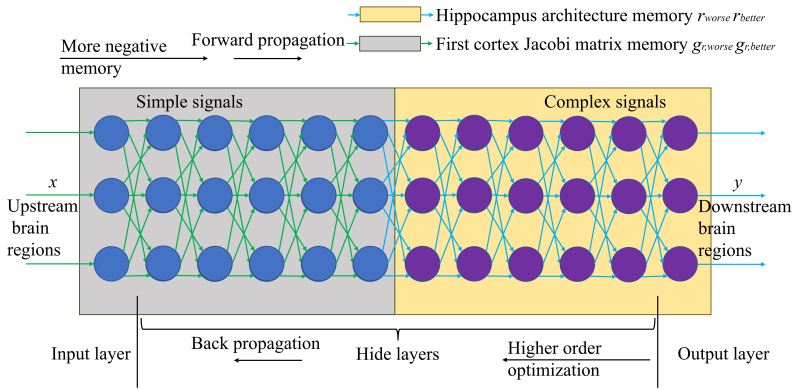


(d)

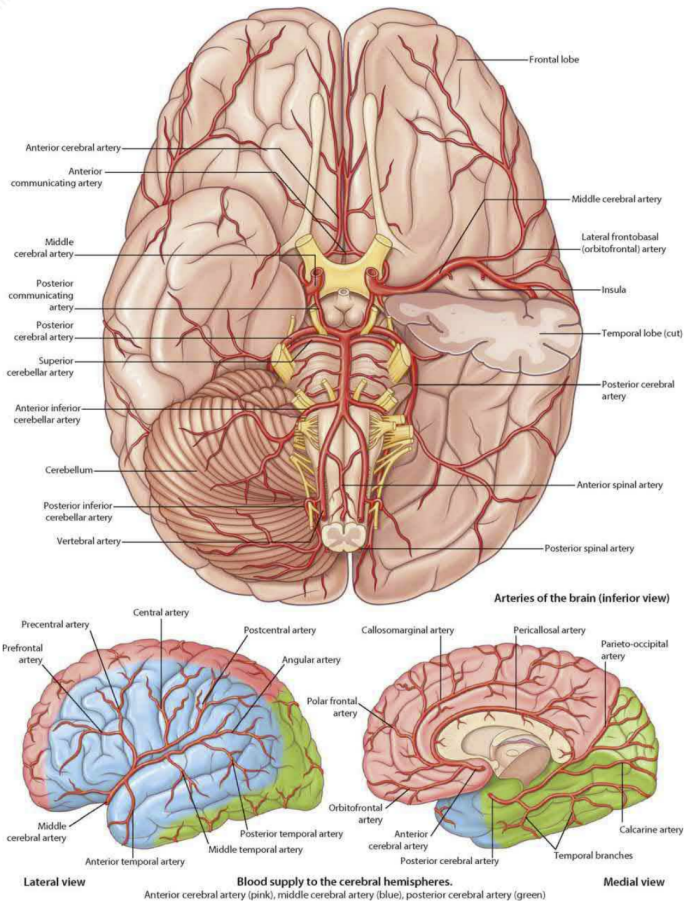


(e)





(h)



(i)

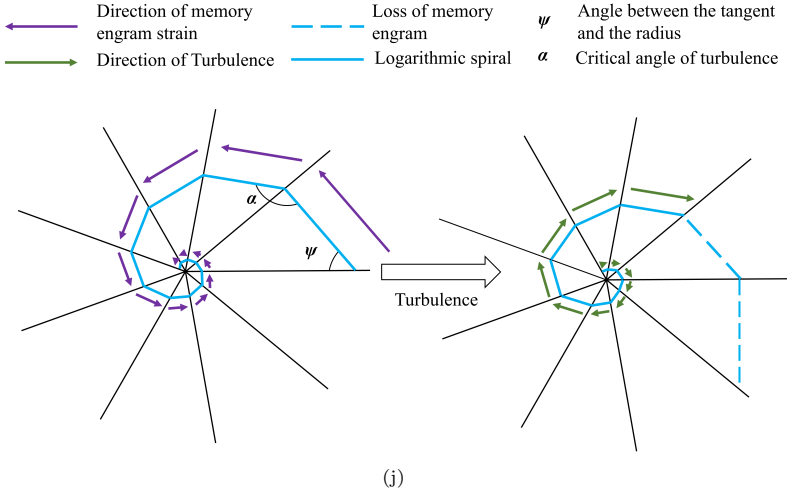


Fig. 1 The brain's reverse turbulence is explained by figures: (a) Biological experiment results [22] (b) Normal IQ (c) High IQ (d) Low IQ (e) *LEN* points of relatively good and inferior memories brains plasticity for quantum computing (f) The critical angle between turbulence and laminar flow and if short-term memory turns to long-term memory [29] (g) Alzheimer's disease (h) Deep learning model for upstream and downstream brain regions (i) Cerebral artery, from *Gray's Atlas of Anatomy 3rd Edition* (j) Angles of logarithmic Spiral and loss of memory engram

Formula (4) updates $r(m, k)$ by current and memory synaptic effective range weight, the best previous $r(m, k)_{best}$. In the model featuring critical period, the hypothesis is best previous brain plasticity affects current brain plasticity. $P = \text{sign}(\text{rand} - 0.5) \times \text{rand} \times (j_{\max} - j) / j_{\max}$ implements plus or minus disturbance of brain plasticity astrocytes phagocytose synapses factor, and this also enables dynamic synaptic strength balance. The dynamic forgotten memory astrocytic synapse formation cortex memory persistence factor and disturbance astrocytes phagocytose synapses factor shown in Fig. 2. $(j_{\max} - j) / j_{\max}$ illustrates we give decreasing weights of factor at critical period in P . $\text{sign}(\text{rand} - 0.5)$ gives Formula P both positive and negative results. P can be negative because of astrocytes phagocytose synapses, but considering the strength rebalance of synaptic effect, P should be positive and negative. The P decreases with the maturation response of astrocytes.

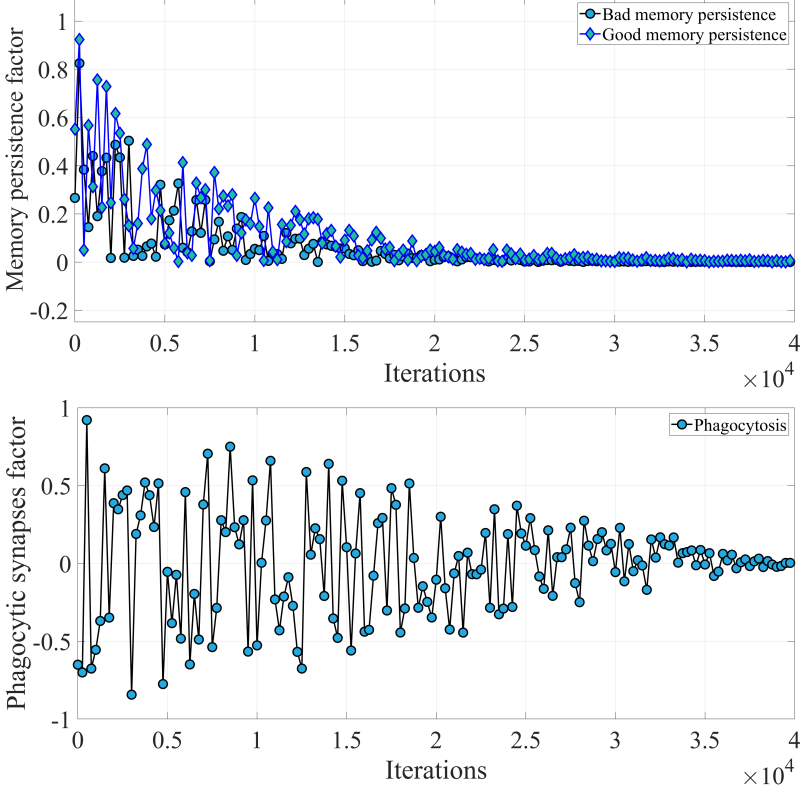


Fig. 2 Astrocytic synapse formation cortex memory persistence factor and astrocytes phagocytose synapses factor: (a) Astrocytic synapse formation cortex memory persistence factor (b) Astrocytes phagocytose synapses factor

In our opinion, when you are considering one problem, whether positive or negative, the exacted working memory brain plasticity may reflect quantum, and exhibit exponential decay of wave function for a while because of barriers in hippocampus and cortices. It is important to maintain inner peace, for reducing these effects of exponential decay, and flatter curve. The actions of neurons may like particles, at the LEN points of relatively good or inferior memories, mapping functions of these extracted memories brains plasticity may be quantum, the square of the amplitude is the distribution probability of the particle by quantum mechanics, and distribution probability of $y = R - r(m, k)_{i,better}$ or $y = R - r(m, k)_{i,worse}$ satisfies $|\Psi[f(y)]|^2 \propto \frac{\exp[-2|f(y)| \times L(t)]}{L(t)}$ or $|\Psi(y)|^2 \propto \frac{\exp[-2|y| \times L(t)]}{L(t)}$. The wave function describes synaptic effective range weights or brain plasticity, The length of time is LEN form $(j - LEN + 1)$ th iteration to j th iteration, and by using Mont Carlo method to calculate $r(m, k)_{temp,worse} = \text{sign}(\text{rand} - 0.5) \times \beta \times |r(m, k)_{best} + \text{rand} \times [r(m, k)_{best} - r(m, k)_{better}] - \sum_{i=j-LEN+1}^j \frac{r(m, k)_{i,worse}}{LEN}| \times \ln(\frac{1}{\text{rand}})$, $L(t) = 2 \times \beta \times |r(m, k)_{best} + \text{rand} \times$

$[r(m, k)_{best} - r(m, k)_{better}] - \sum_{i=j-LEN+1}^j \frac{r(m, k)_{i, worse}}{LEN} |, r(m, k)_{temp, better} =$
 $\text{sign}(rand - 0.5) \times \beta \times |r(m, k)_{best} + rand \times [r(m, k)_{best} - r(m, k)_{better}] -$
 $\sum_{i=j-LEN+1}^j \frac{r(m, k)_{i, better}}{LEN} | \times \ln(\frac{1}{rand}), L(t) = 2 \times \beta \times |r(m, k)_{best} + rand \times$
 $[r(m, k)_{best} - r(m, k)_{better}] - \sum_{i=j-LEN+1}^j \frac{r(m, k)_{i, better}}{LEN} |, \beta = 1,$ and β is shrinkage-expansion coefficient, a superposition of wave function of time. The length of time LEN , it may be short-term memory in quantum computing. j is current iteration. i is i th iteration. $MW_2 \times Q_N + MW_3 \times Q_P$ means a linear superposition of two wave functions. $r(m, k)_{i, better}$ is relatively good synaptic effective range weight in i th iteration, $r(m, k)_{i, worse}$ is relatively inferior synaptic effective range weight in i th iteration, $r(m, k)_{i, best}$ is best previous synaptic effective range weight in i th iteration. And $(rand > 1/2)$ means it has $2^2 = 4$ scenarios of the relatively inferior and good two-qubit: $\{1, 1\}$, $\{1, 0\}$, $\{0, 1\}$ or $\{0, 0\}$. The quantum uncertainty of relatively inferior and good range weights, because of scan resolution of the cortical folds. The effects of astrocytes phagocytose synapses P and quantum computing Q in calculations are very similar in minus or plus, the process of astrocytes phagocytose synapses may a normal computer by random or gradient, but also a quantum computer. It may be that the process of astrocytes phagocytose synapses is driven by positive and negative memory of brain plasticity, by excitatory/inhibitory interactions. The quantum computing to update the synaptic effective range weights by short-term memory, means $r(m, k)_{temp, better}$ or $r(m, k)_{temp, worse}$.

We can imagine our brain as the earth, and the production of geocentric lava occurs like short-term memory happen in the hippocampus, and the process is quantum. Earthquakes on the surface are released due to potential energy, just as strong short-term memory is selected and turns to long-term memory, and is stored in memory engram cells of different cortices, can be released.

Referring formula (2) and (4), the memory consolidation formula (4) can be shown as follows, it is the relationship of working memory and long-term memory, and maximum of directional derivatives is gradient. From hippocampus to cortices, it is achieved from non-classical to classical in brain. Long-term memory is gradient of brain plasticity $\frac{\partial r}{\partial \bar{n}}$ which is too idealistic, there is an angle $\alpha_c = \tan^{-1} \frac{\frac{\partial r}{\partial \bar{n}}}{\frac{\partial r}{\partial t}}$, α_c will increase because of human aging, the angle α_c is the critical value, greater than it is turbulence and less than it is laminar flow. And turbulence becomes laminar flow gradually throughout aging, the $\alpha_c = \tan^{-1} \frac{\frac{\partial r}{\partial \bar{n}}}{\frac{\partial r}{\partial t}}$ was shown in Fig.1(f) [29]. If $\alpha_c \geq \pi$, symptoms of Alzheimer's disease will appear, and atrophy and hardening of the hippocampus because of reverse turbulence, was shown in Fig. 1(g), just like a star dying to form black hole. Our conjecture is Alzheimer's disease cognitive impairment is caused by search direction reversal, the negative gradient of Back propagation is modified by positive gradient, and unable to converge, change of direction of transition was shown in Fig. 1 (f)-(g) [29]. The $\tan \alpha_c$ in formula (4) is equivalent to MW_1 or MW_2 or MW_3 in formula (2). The simultaneous interaction of two different

turbulence directions of $\alpha_c \geq \pi$ memory loss and $\alpha_c \leq \frac{\pi}{2}$ memory consolidation leads to β -amyloid plaques in brain. But the positive gradient of BP might be the more important reason for Alzheimer's disease than β -amyloid plaques in brain.

We studied Alzheimer's disease based on turbulence in brain information transmission and dysfunction of the neurotransmitter system. Disorders of neurotransmitters lead to abnormalities in turbulence between cortexes inside the brain - that is, the reverse turbulence. First we look at the arteries of the healthy brain Fig. 1(i), where the large and middle cerebral arteries are located inside the brain, and then the external branch arteries of the brain turn to small. The brain undergoes turbulent movements beyond a minimum critical value to spread information from the internal large and middle arteries to the small external branch arteries, that is, normal turbulence is from the downstream brain regions of the internal cortices to the upstream brain regions of the external cortices to achieve the Back propagation of Deep learning. Similarly, the large and middle aqueducts connecting the internal cortices are also larger in the downstream brain regions of the brain, while the aqueducts in the upstream brain regions of the external cortices are smaller.

For example, staying up late on the function of the kidneys and liver, and affects the excretion of intestinal toxins, so that the blood accumulates too many toxins and garbage and affects the metabolism of the brain. The blood and toxins are transmitted to the large and middle arteries of the brain through cardiac contraction, so that the large middle arteries appear cerebral atherosclerotic plaques and infarction, in order to unblock the plaques of these large and middle arteries, the heart must use a larger systolic blood pressure may lead to systolic hypertension. Similarly, because β amyloid and tau proteins affect the cerebrospinal fluid, which in turn affects the large and middle aqueducts of the internal cortices. In this way, the branch arteries external our brain and the branch aqueducts between the cortices are relatively large because there is no garbage and toxins, while the large middle arteries inside the brain and the large and middle aqueducts in the cortices are relatively small. As a result, there is a reverse diffusion of turbulence between the cortices.

Heart failure is another condition in which reduced blood flow makes the large middle artery and large middle aqueduct in the downstream brain regions relatively small.

Increased systolic blood pressure due to atherosclerosis, systolic hypertension, and heart failure leading to decreased blood flow and the large middle arteries in the brain turn to small, which may be responsible for Alzheimer's disease.

Why do patients with Alzheimer's disease have circadian rhythm disorders, after the patient lies down, because only a smaller systolic blood pressure than the original can clear the large middle aqueducts inside the brain β -amyloid and tau protein and toxins and garbage of the large middle arteries, lying down also increases blood flow and expands the large middle artery and large middle aqueduct, so that the direction of partial turbulence inside the brain returns

to normal, makes thinking clear and memory restored and constant thinking, which in turn leads to circadian rhythm disorders.

Brain dynamics analogous to river dynamics, when the river that flows backwards, because the previous river flow slope is opposite to the current flow slope, it may lead to river siltation. The river siltation is similar to β -amyloid plaques in brain. The river that flows backwards is similar to turbulence reverses in downstream brain regions.

$$\begin{aligned}
\frac{\partial r}{\partial \vec{n}}|_{(x_0, y_0)} &= \frac{\partial r}{\partial x} \cos \alpha + \frac{\partial r}{\partial y} \cos \beta|_{(x_0, y_0)} \\
&= \left(\frac{\partial r}{\partial x}, \frac{\partial r}{\partial y} \right)|_{(x_0, y_0)} \cdot (\cos \alpha, \cos \beta) \\
&= \text{grad } r(x_0, y_0) \cdot (\cos \alpha, \cos \beta) \\
&= \text{grad } r(x_0, y_0) \cdot \vec{e}_n \\
\text{if } \alpha = 0, \vec{e}_n &= (1, 0) \text{ then } \max \frac{\partial r}{\partial \vec{n}}|_{(x_0, y_0)} = \nabla r(x_0, y_0) \\
\text{or } \frac{\partial r}{\partial \vec{n}}|_{(x_0, y_0, z_0)} &= \frac{\partial r}{\partial x} \cos \alpha + \frac{\partial r}{\partial y} \cos \beta + \frac{\partial r}{\partial z}|_{(x_0, y_0, z_0)} \\
&= \left(\frac{\partial r}{\partial x}, \frac{\partial r}{\partial y}, \frac{\partial r}{\partial z} \right)|_{(x_0, y_0, z_0)} \cdot (\cos \alpha, \cos \beta, \cos \gamma) \\
&= \text{grad } r(x_0, y_0, z_0) \cdot (\cos \alpha, \cos \beta, \cos \gamma) \\
&= \text{grad } r(x_0, y_0, z_0) \cdot \vec{e}_n \\
\text{if } \alpha = 0, \vec{e}_n &= (1, 0, 0) \text{ then } \max \frac{\partial r}{\partial \vec{n}}|_{(x_0, y_0, z_0)} = \nabla r(x_0, y_0, z_0) \\
\text{or } \alpha_c &= \tan^{-1} \frac{\frac{\partial r}{\partial \vec{n}}}{\frac{\partial r}{\partial t}} \\
\vec{e}_n &= (\cos \alpha_c, \sin \alpha_c, 0) \\
\text{if } \alpha &\geq \alpha_c \text{ turbulence, short - term memory turns to long - term memory} \\
&\text{else } \alpha \leq \alpha_c \text{ laminar flow, no long - term memory can be transited} \\
&\text{by short - term memory}
\end{aligned} \tag{4}$$

The pseudocode of PNN is as follows, which encompasses Forward and Back Propagation.

Because it is the reverse turbulence downstream of the brain, the positive gradient of renewal synaptic effective range is mainly distributed near the downstream brain regions of the internal cortices of the brain. The positive gradient of the connecting weights may be related to the reverse turbulence of immune cells leading to neuroinflammation. The n th to $n + m$ th layers of the downstream brain regions use redundant objective function information of the $n + j$ th to $n + m + j$ th layers of the downstream brain regions.

Require: initialization parameter: generation of randomly connection weight $w(m,k)$, neuron m , synapse k , **and** effective range weight $r(m,k)$

#1Do $j=1:j_max$ (j_max is maximum iterations)

#2While the condition of loss function is satisfied, it stops iterating

#3Do $g=1:m_max$ (m_max is number of neurons)

Using the memory best previous solution to update the $w(g,k)$ and $g_r(m,k)$ **While** it satisfies the conditions Update $r(m,k)$ at formula (4) by current **and** memory synaptic effective range weight **for** brain plasticity **and** implements plus **or** minus disturbance of brain plasticity— P , astrocytes phagocytose synapses factor at critical period, it also considers quantum computing **and** short-term memory through $MW_1 \times R + MW_2 \times Q_N + MW_3 \times Q_P$ to update $r(m, k)$

#4Do $m=1: m_max$

#5Do $k=1: k_max$ (k_max is synapse population)

#6Do $t=n_3(m,k):n_3(m,k+1)$ (t is time point)

When Back Propagation position moves from $n_3(m,k)$ to $n_3(m,k+1)$, update synaptic connection weight at Formula (1) $w(g,k)$, synaptic effective range weight at Formula (2) $r(m,k)$ **for** competition by the current gradient informational **and** memory positive **and** negative gradient informational synapse formation **and** consider the forgotten memory— M , astrocytic synapse formation cortex memory persistence factor at critical period.

#6End do

#4End do

#5End do

Update weights of synaptic connections **and** effective ranges, **then** Forward Propagation is performed to obtain loss

Then result of Back Propagation updates the neutron s synaptic position by Formula (3) $n_1(m,k)$ **for** strength rebalance

#3End do

#2End while

#1End do

*As for updating $w(g,k)$ and $r(m,k)$, the global synaptic effective range weights $r(m,k)$ need to be changed by overall optimization, while the same type of connection weight $w(g,k)$ just needs to be changed by local optimization. i.e., research on disease dynamics, when infection rates (or cure rates) change, the time interval of the infection rate and cure rates both need to be updated at the same time.

Then loops and iteration of Deep learning, an early iteration of the Back propagation is negative gradient which used to update synaptic connection weights and range weights. Then the later iteration of Back propagation gradually becomes half negative gradient and half positive gradient, canceling out the excitement of the synapses, half of the $n + m$ th layers of the downstream brain regions use redundant objective function information of the downstream brain regions, and half of the $n + m$ th layers of the downstream brain regions use the objective function information of the normal upstream brain regions, so that the synapse loss and hallucinations of Alzheimer’s disease occurs.

If the Back propagation at the beginning of the iteration is negative gradient, the Back propagation in the middle of the iteration gradually becomes half negative gradient and half positive gradient, half of the $n + m$ th layers of the downstream brain regions use redundant objective function information of the downstream brain regions, and half of the $n + m$ th layers of the downstream brain regions use the objective function information of the normal upstream brain regions, to reflect the synapse loss and hallucinations in early Alzheimer’s disease, and the Back propagation in the late iteration is positive gradient and the n th to $n + m$ th layers all use the objective function information of redundant downstream brain regions, to reflect more severe Alzheimer’s cognitive impairment. The model realized the early synapse loss and hallucinations in Alzheimer’s disease to more severe cognitive impairment in the later stage.

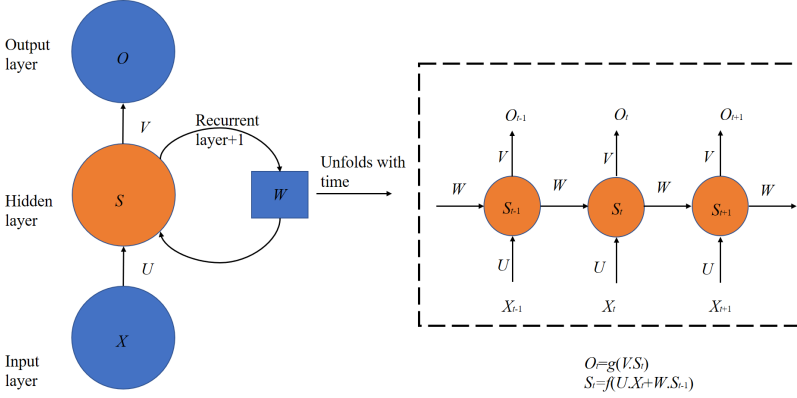
The reverse turbulence affects memory engrams, the reverse turbulence has a certain effect on the memory engrams in the middle of iteration, and reverse turbulence has a greater effect on the memory engrams in the late iteration.

3 Discussion

3.1 Comparison of PNNs in some scenarios

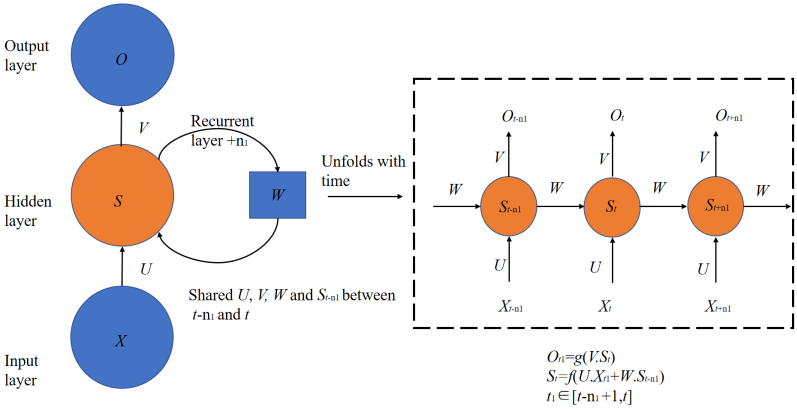
Parameters regarding the abovementioned test is as follows: testing environment is WIN11 and MATLAB2020a, the parameters for updating the weights remain the same for the three tests, and the number of iterations is $j_{\max} = 40000$. The tests employ cosine filter, in which input are filter from point $t + 1$ to $t + 4$, and prediction of output is filter at $t + 5$ point. $l_{\min} = 2$, $k_{\max} = 9$, $l_{\max} = 44$. Memory ensembles of long-term memory produced once each iteration. but retrieval processes of short-term memory happened once by many iterations. Three methods were all considered the memory the best previous solution, so RRPNN and ORPNN both take into consideration the current and memory connection weight and synaptic effective range. But CRPNN only pays heed to the current and memory connection weight, as the synaptic effective range remains constant in synapse formation. Only ORPNN takes into account the current gradient informational and memory positive and negative gradient informational synapse formation, and it also considers current and memory brain plasticity. In the Fig.4, the ORPNN model includes two scenarios, in addition to astrocytes phagocytose synapses factor, one only considering the best previous memory of synapse formation ORPNN-MF(P)-PF,

RNN flow chart



(a) RNN U is the weight from the input layer to the hidden layer, V is the weight from the hidden layer to the output layer, S is the vector of the hidden layer, X is the vector of the input layer, and O is the vector of the output layer. W is the connection weight.

CRPNN and RRPNN flow charts

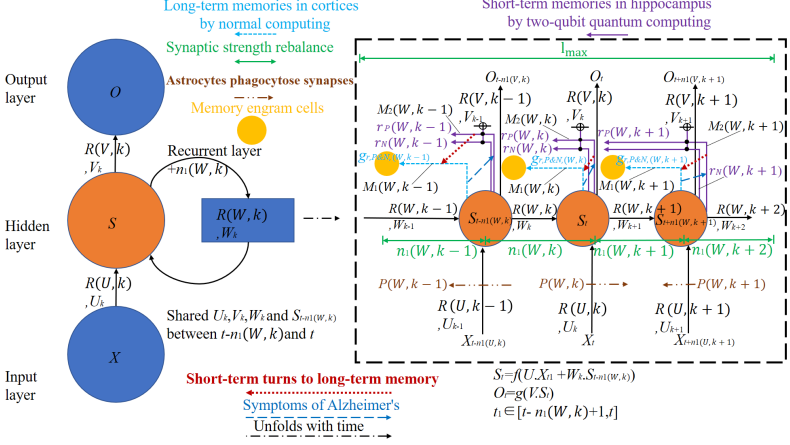


(b) CRPNN and RRPNN CRPNN is very similar to RNN, except that the iteration time is changed from +1 to +n₁. The n₁ in RRPNN is a variable, and the length of n₁ is randomly generated within a certain range.

and the other considering both the best previous memory and the relatively inferior memory of synapse formation ORPNN-MF(P&N)-PF. MF(P) represents positive cortex memory persistence, and MF(P&N) represents positive and negative cortex memories persistence.

Fig.3 shows respectively the flow charts of RNN, CRPNN, RRPNN and ORPNN

ORPNN flow chart



(c) ORPNN Shared weights $U_k, V_k, W_k, R(W, k)$ and $S_t - n_1(W, k)$ between $t - n_1(W, k)$ and t , where $R(W, k)$ is the synaptic effective range weight. Astrocytes phagocytose synapses factor $P(W, k)$ realizes synaptic phagocytose, k is taken as $1 - k_{\max}$ to represent different synapses, and k_{\max} is the size of synapse population. $n_1(W, k)$ is the synaptic effective range of the variable W and synapse k . Take positive or negative values to make $\sum_{k=1}^{k_{\max}} P(W, k) = 0$ achieve dynamic balance of synapses. The time length of $\sum_{k=1}^{k_{\max}} n_1(W, k) = l_{\max}$ achieves the static balance of synapses. l_{\max} represents the sum of synaptic effective ranges. The cortex memory persistence factor $M(W, k)$ gets positive and negative memories in memory engram cells with the best previous gradient information and relatively inferior and good gradient information of synapse formation- $g_{r, P \& N}$, long-term memory. Another memory persistence factor $M(W, k)$ gets positive and negative memories with the relatively inferior and good brain plasticity- r_P and r_N , short-term memory, which through quantum computing.

Fig. 3 CRPNN, RRPNN and ORPNN flow charts.

A total of 3 tests were conducted, with the results shown in Fig.4, in which the results of the variation of the logarithm of the loss of PNN with iterations are also provided.

Result of the first test: the correlation coefficient between CRPNN simulation data and actual data is 0.8057, the correlation coefficient between RRPNN simulation data and real data is 0.8706, and the correlation coefficient between M(P)ORPNN and M(P&N) ORPNN simulation data and real data are 0.9709 and 0.9687. Result of the second test: the correlation coefficients are 0.8292, 0.8921, 0.9668 and 0.9646 respectively. Result of the third test: the correlation coefficients are 0.8031, 0.8728, 0.9622 and 0.9588 respectively.

The results of the RRPNN test turned out to be satisfactory, and though the connection weights are updated by equation (1) and the memory the best previous solution, more satisfactory optimization results could be found for random synaptic effective range locations.

The ORPNN showed strong fluctuation in the iterations, whereas the final convergence turned out better and faster than the RRPNN and the CRPNN.

Iteration of CRPNN is not convergent. RRPNN has slow convergence.

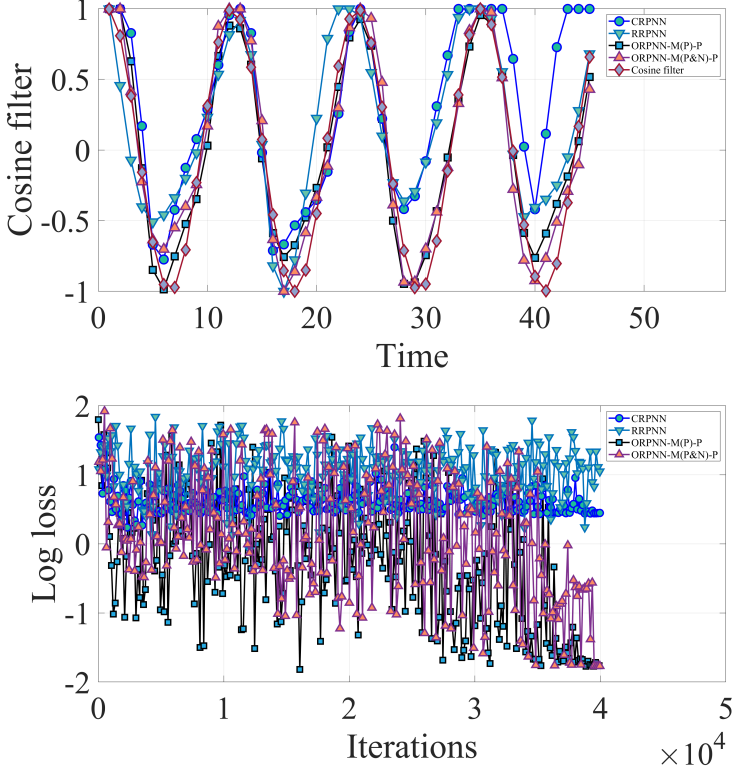


Fig. 4 first test results belong to CRPNN, RRPNN, and ORPNN respectively

The number of iterations is $j_{\max} = 40000$. In order to study the effect of the astrocytic synapse formation cortex memory persistence factor and astrocytes phagocytose synapses factor, Fig.7 is obtained. In the first scenario of ORPNN-PF, only the astrocytes phagocytose synapses factor is taken into account with the best previous $r(m, k)_{best}$ and a correlation coefficient of 0.9515. The second scenario ORPNN-MF(P)-PF takes into account both the astrocytic synapse formation positive memory persistence factor in formula (2) and astrocytes phagocytose synapses factor in formula (4), cortex memory persistence factor considers positive memory. It may have better results and a correlation coefficient of 0.9573 at critical period. The third scenario ORPNN excludes the astrocytic synapse formation cortex memory persistence factor and astrocytes phagocytose synapses factor at the closure of critical period then astrocytes become mature. It may have worst results a correlation coefficient of 0.9208. The fourth scenario ORPNN-MF(P) only the astrocytic synapse formation positive cortex memory persistence factor is taken into account with the gradient of the best previous $g(m, k)_{best}$ and a correlation coefficient of 0.9346. The fifth scenario ORPNN-MF(P&N)-PF takes into account both the astrocytic synapse formation cortex memory persistence factor in formula (2) and

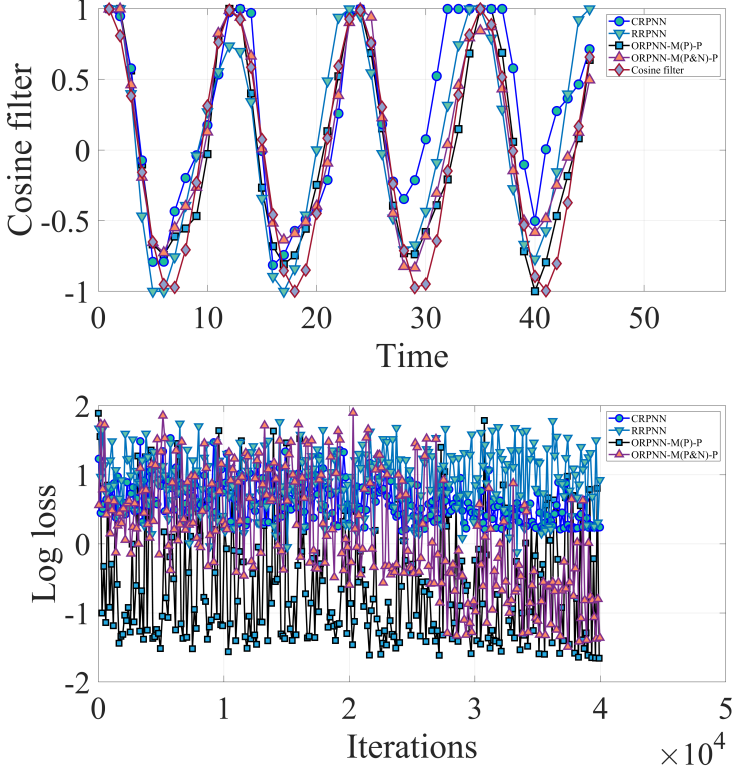


Fig. 5 second test results belong to CRPNN, RRPNN, and ORPNN respectively

astrocytes phagocytose synapses factor in formula (4), cortex memory persistence factor considers positive and negative memories. It may have best results and a correlation coefficient of 0.9646 at critical period. In Fig.7, P means astrocytes phagocytose synapses factor, M(P&N) means positive and negative cortex memories persistence factor, M(P) means positive cortex memory persistence factor.

3.2 Synapse formation affects brain function - inhibiting dendrites

We then modified the ORPNN model accordingly for analysis. By modifying l_{\min} , we managed to simulate the process of brain cognition from infancy to the senile phase. l_{\min} exhibits elasticity at the beginning as a decimal value, then gradually decreases in plasticity. In this way the increase in minimum synaptic effective range from $l_{\min} = 2$ to $l_{\max}/k_{\max} \approx 5$ made diversity of synaptic effective range progressively smaller. CRPNN corresponds to the senile phase period of brain cognition as it satisfies $l_{\min} = l_{\max}/k_{\max} = 44/9 \approx 5$, and the funny thing is that the iteration is not convergent at CRPNN.

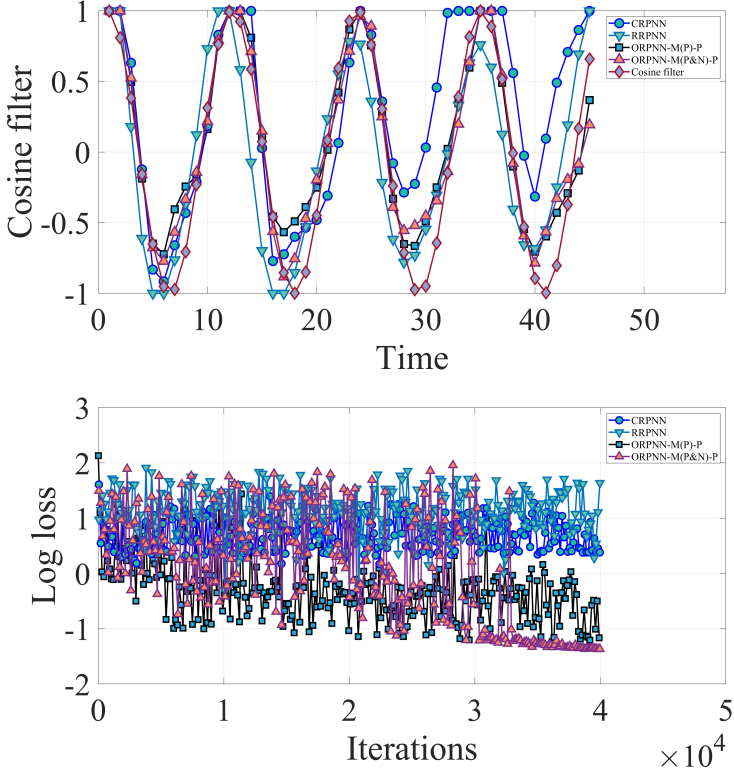


Fig. 6 third test results belong to CRPNN, RRPNN, and ORPNN respectively

We obtained a possible explanation to the research findings of Dr. Luo’s team through PNN. We drew the relationship of different l_{\min} (minimum synaptic effective range), different k_{\max} (synapse population) and correlation coefficients, and the results are shown in Fig. 8 below. We also conducted another test, in which the cosine filter and cycle gradually diminish by time-variable cycle cosine filter, and the number of iterations is $j_{\max} = 80000$. The functions of dendrites are to receive and process signals from other neurons. Our simulation results reveal that synapse formation will inhibit dendrites to a certain extent, furthering the findings of Dr. Luo’s team at the Stanford University. An explanation to this is that synaptic growth will lead to a reduction in the changes in synaptic effective range, and an overgrowth will inevitably disrupt the diversity and plasticity of human brain. $l_{\min} = 2 - 5$, $k_{\max} = 7 - 9$. Fig.8 concerns the relationship between synapse formation and correlation coefficients in ORPNN. The synapse formation could involve a decrease in k_{\max} and an increase in l_{\min} . The PNN situation can be thought as the Finite Element Method, in which neurons of the brain can be regarded as nodes of FEM. As increased in the number of nodes and finer meshes can lead to more accurate computational results of FEM, more neurons and smaller minimum

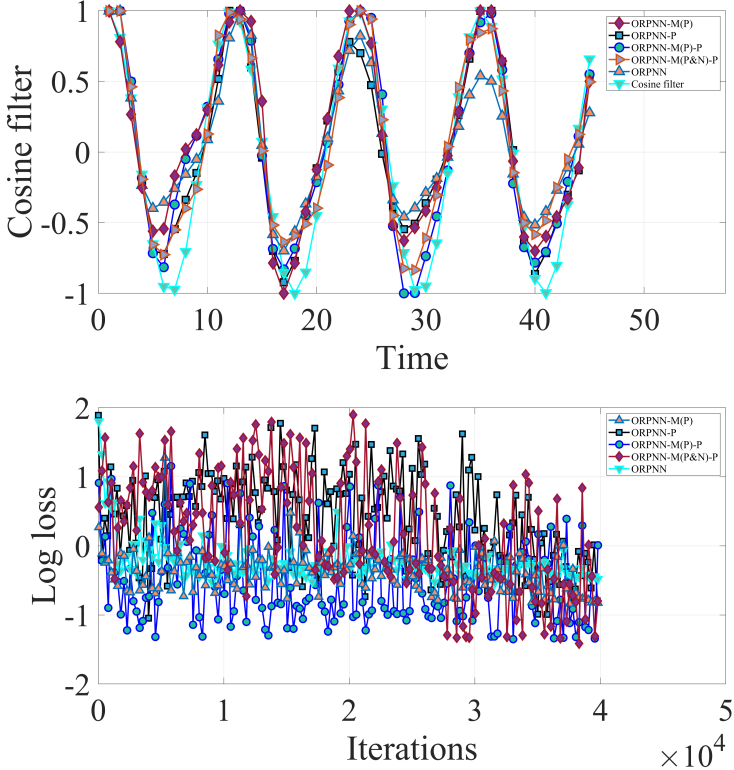


Fig. 7 Simulations at critical periods and the end of critical periods

synaptic effective range can also help us obtain more desirable and accurate PNN results. When synapse population k_{\max} decreases and sum of synaptic effective ranges l_{\max} is a constant, the diversity of local synaptic effective range may be improved as the synaptic effective range enlarges from l_{\min} to l_{\max}/k_{\max} , so k_{\max} decreases may enhance correlation coefficients by accident, as you can observe from Fig. 9 (a) $l_{\min} = 3 - 4$, $k_{\max} = 7 - 8$ and Fig. 9 (b) $l_{\min} = 2 - 3$, $k_{\max} = 7 - 9$. When the minimum synapse length is too small, the probability of local synaptic accumulation increases, which also affects the optimization results, It can be seen from Table 2.

3.3 Effects of astrocytes are reflected in astrocytes phagocytose synapses factor and cortex memory persistence factor during critical and closure critical period

As for the ORPNN-MF(P)-PF situation (ORPNN both containing astrocytic synapse formation positive cortex memory persistence factor and astrocytes phagocytose synapses factor at critical period), synaptic effective ranges with

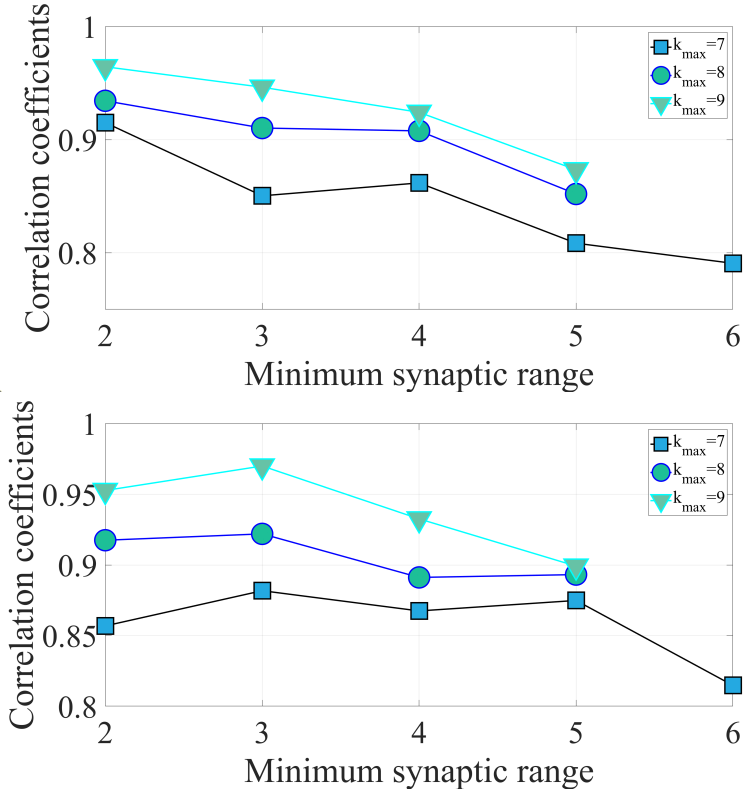


Fig. 8 Relationship between synapse formation (different l_{\min} and k_{\max}) and correlation coefficients: (a) ORPNN-M(P)-PF, (b) ORPNN-PF

different l_{\min} and different input variables are provided in Table 1. When $l_{\min} = 5$, the synapse grows to a certain extent, and synaptic effective range remains almost the same, thus leading to a worsened simulation result. When the synapse grows, standard deviation of synaptic effective range at the end of the iteration diminishes, and the correlation coefficients decreases to a certain extent when $l_{\min} = 5$. From $l_{\min} = 2$ to $l_{\min} = 5$, synaptic effective range gradually loses its diversity and plasticity. The number of iterations is $j_{\max} = 80000$. And the results of synaptic effective range and correlation coefficient when iteration equals 20,000, 40,000, 60,000 and 80,000 were also observed, as 4444 in Table represents the synaptic effective ranges are all 4, and 0.9641, 0.9683, 0.9683 and 0.9645 are the correlation coefficients when iteration equals 20,000, 40,000, 60,000 and 80,000, respectively.

As for the ORPNN-PF situation (ORPNN only containing astrocytes phagocytosis synapses factor), synaptic effective ranges with different l_{\min} and different input variables are provided in Table 2.

Comparing with the other Tables, the effect of astrocyte made local synaptic effective range remain in an appropriate length at critical period, as one can observe in Tables 1, 3, 4 and 5. Else some synapses have longer length and

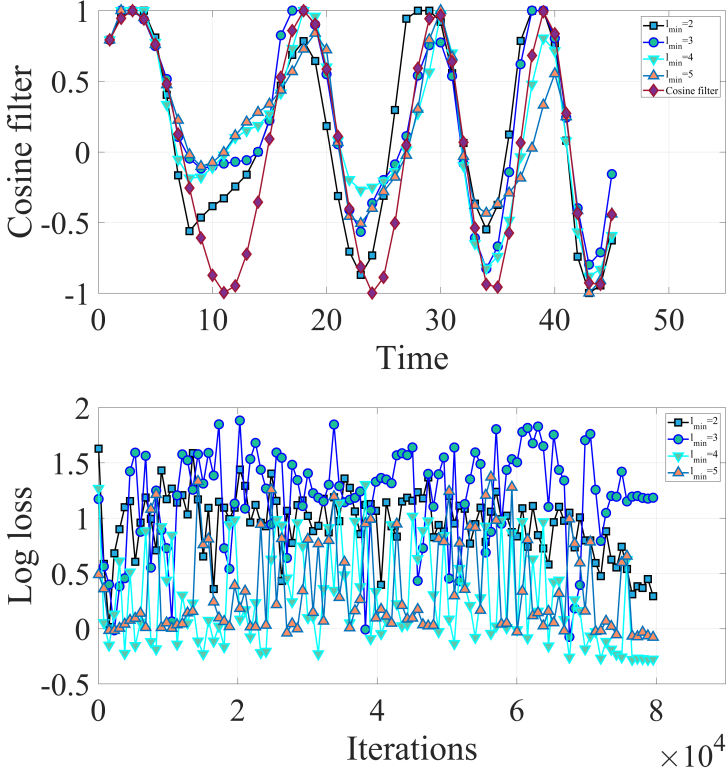


Fig. 9 ORPNN test results are $l_{\min} = 2 - 5$ and $k_{\max} = 9$ respectively (a)ORPNN

disorder, resulting in the alignment of other synaptic effective ranges, as one can observe in Table 2. The simulations in Tables similar to that failure to the closure of critical period results in neurodevelopmental disorders, and then astrocytes become mature [19]. The calculation of the correlation coefficient was better than that of Tables 2, 4 and 5 but worse than Table 3 at critical period, as model of Deep Learning contains both astrocytic synapse formation cortex memory persistence factor and astrocytes phagocytose synapses factor in Table 1 and Fig.10(b).

Table 2 shows that the local accumulation of synapse length is accompanied by Vanishing Gradients by Fig.9 and Tables. It can be seen from Table 2 that activity of synapse formation gradually diminishes with iterations and growth of the l_{\min} , the calculation of the correlation coefficient in Table 2 also turns out worse than in other Tables.

For Table 3 which considers only astrocytes phagocytose synapses factor, synapse formation showed good activity with iterations and l_{\min} growth. We can find better results of correlation coefficients in Tables respectively. As the probability of Vanishing Gradients is small when considering astrocytes phagocytose synapses factor by Fig.11(c) and Tables, the result of Table 3

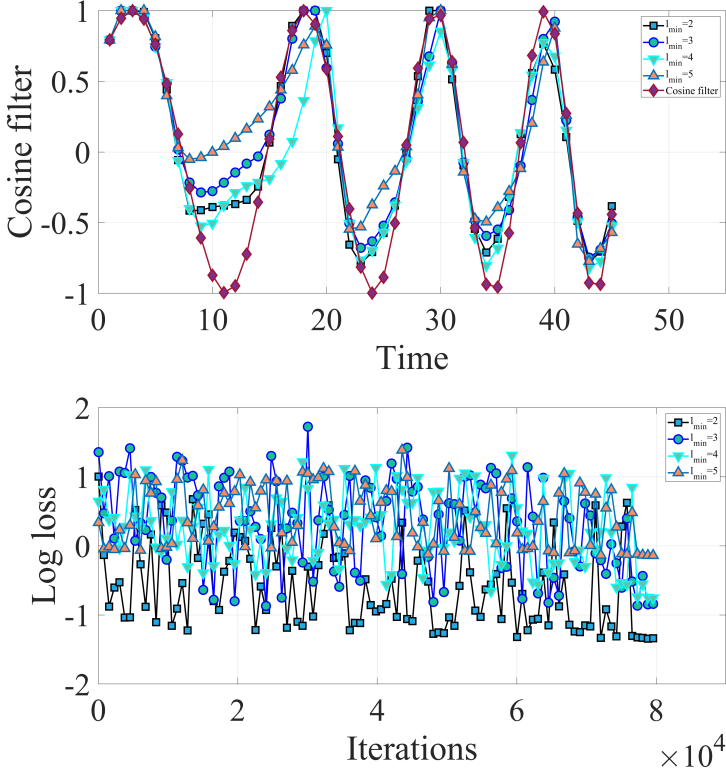


Fig. 10 ORPNN test results are $l_{\min} = 2 - 5$ and $k_{\max} = 9$ respectively (b)ORPNN-MF(P)-PF

converges even at $l_{\min} = 5$, while that of other Tables converge poorly at $l_{\min} = 5$.

Table 4 only deals with the cortex positive memory persistence factor, which maintains the slow change in synapse length, and the synapse formation shows a worse activity with iterations and minimum synaptic effective range growth than in Tables 1-3 and 5. The Vanishing Gradients of the positive cortex memory persistence factor is worse than that of Tables 1, 3 and 5, and better than that of Table 2 by Fig.12(d) and Tables.

Table 5 deals with the positive and negative cortex memories persistence factor, which maintains the active change of synapse length, and the synapse formation shows a better activity with iterations and minimum synaptic effective range growth than in Tables 1 and 3. The Vanishing Gradients of the positive and negative cortex memories persistence factor is worse than that of Tables 1 and 3, and better than that of Table 2 and 4 by Fig.13(e) and Tables.

When $l_{\min} \approx l_{\max}/k_{\max} = 44/9 \approx 5$, similar to the case of CRPNN, it can be seen from Tables 1-5 that the correlation coefficient effect is not so good at this time, and even Tables 1, 2, 5 is less ideal.

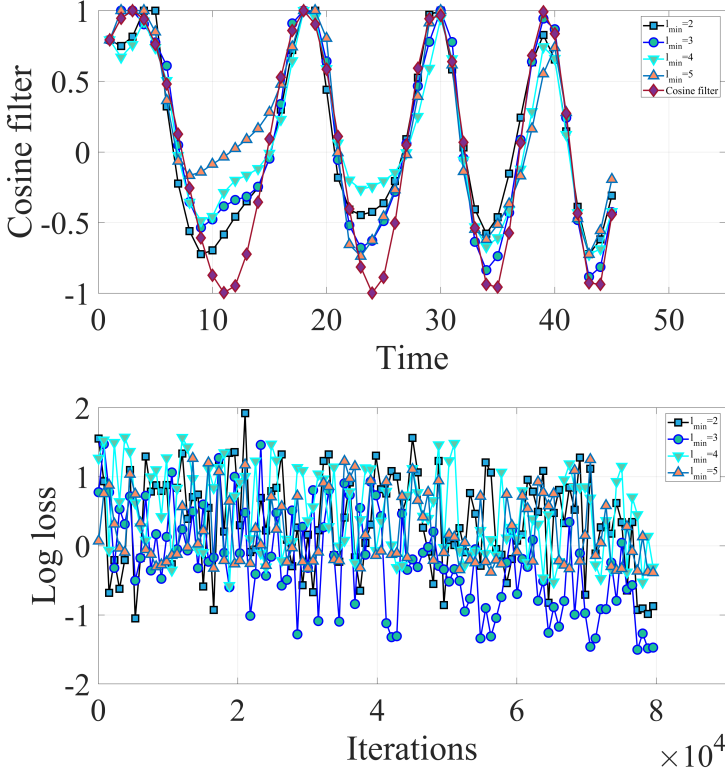


Fig. 11 ORPNN test results are $l_{\min} = 2 - 5$ and $k_{\max} = 9$ respectively (c)ORPNN-PF

ORPNN contains both astrocytic synapse formation positive cortex memory persistence factor and astrocytes phagocytose synapses factor-ORPNN-MF(P)-PF. We propose the simulation of $l_{\min} = 2-5$ and $k_{\max} = 9$ respectively, and the correlation coefficients are 0.9645, 0.9464, 0.9242 and 0.8734 respectively. ORPNN contains neither astrocytic synapse formation cortex memory persistence factor nor astrocytose phagocytose synapses factor at the closure of critical period-ORPNN, and the correlation coefficients are 0.8730, 0.9282, 0.8846 and 0.8579 respectively. ORPNN only contains astrocytes phagocytose synapses factor-ORPNN-PF, and the correlation coefficients are 0.9527, 0.9700, 0.9326 and 0.8992 respectively. ORPNN only contains astrocytic synapse formation positive cortex memory persistence factor with positive memory - ORPNN-MF(P), and the correlation coefficients are 0.9382, 0.9265, 0.9115 and 0.8663 respectively. ORPNN only contains astrocytic synapse formation cortex memory persistence factor with negative and positive memories-ORPNN-MF(P&N), and the correlation coefficients are 0.9592, 0.9423, 0.9228 and 0.8878 respectively. Different l_{\min} affects simulations can be observed in Fig.9-13. The number of iterations is $j_{\max} = 80000$.

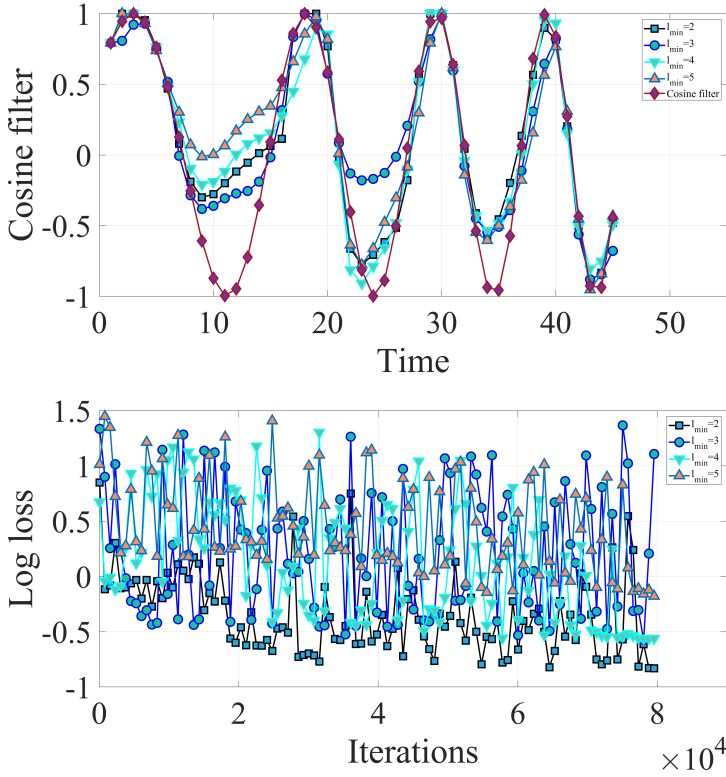


Fig. 12 ORPNN test results are $l_{\min} = 2-5$ and $k_{\max} = 9$ respectively. (d)ORPNN-MF(P)

Table 1 Synaptic effective range with different l_{\min} and different variables-brain plasticity ORPNN-MF(P)-PF, test results are $l_{\min} = 2-5$ and $k_{\max} = 9$ respectively

| | V.L. | S.L. | | | | | | | | | | Std | correlation coefficients |
|----------------|------|------|------|------|------|------|------|------|------|----------------|--------|--------|--------------------------|
| | | S.1 | S.2 | S.3 | S.4 | S.5 | S.6 | S.7 | S.8 | S.9 | | | |
| $l_{\min} = 2$ | V.1 | 5555 | 7777 | 4444 | 6666 | 4455 | 4444 | 4444 | 6666 | 4433 | 1.2693 | 0.9641 | |
| | V.2 | 5545 | 5555 | 5555 | 4444 | 5555 | 5555 | 6666 | 5555 | 4454 | 0.6009 | 0.9683 | |
| | V.3 | 4555 | 6666 | 4444 | 3433 | 4444 | 5555 | 4444 | 6666 | 8677 | 1.2693 | 0.9863 | |
| | V.4 | 6666 | 4444 | 5444 | 6666 | 4444 | 4444 | 7666 | 6666 | 2454 | 1.0541 | 0.9645 | |
| $l_{\min} = 3$ | V.1 | 5555 | 4444 | 4444 | 5555 | 6666 | 6666 | 5555 | 5555 | 4444 | 0.7817 | 0.9409 | |
| | V.2 | 5555 | 6666 | 5555 | 5555 | 5555 | 4444 | 5555 | 5555 | 4444 | 0.6009 | 0.9456 | |
| | V.3 | 6555 | 6666 | 4444 | 6666 | 5555 | 5555 | 4444 | 5555 | 3444 | 0.7817 | 0.9456 | |
| | V.4 | 4444 | 5555 | 5555 | 5555 | 5555 | 5555 | 5555 | 5555 | 5555 | 0.3333 | 0.9464 | |
| $l_{\min} = 4$ | V.1 | 5555 | 4444 | 5555 | 5555 | 5666 | 5555 | 4444 | 5566 | 6544 | 0.7817 | 0.9033 | |
| | V.2 | 5555 | 5444 | 5555 | 5554 | 5555 | 5555 | 5656 | 5555 | 4455 | 0.6009 | 0.9267 | |
| | V.3 | 5655 | 5555 | 5444 | 4444 | 5455 | 6666 | 5555 | 5555 | 4555 | 0.6009 | 0.9258 | |
| | V.4 | 5444 | 5555 | 5666 | 4555 | 5444 | 5555 | 5555 | 6666 | 4444 | 0.7817 | 0.9242 | |
| $l_{\min} = 5$ | V.1 | 5 | 5 | 5 | 5 | 5 | 5 | 5 | 5 | 4 ¹ | 0.3333 | 0.8759 | |
| | V.2 | 5 | 5 | 5 | 5 | 5 | 5 | 5 | 5 | 4 | 0.3333 | 0.8759 | |
| | V.3 | 5 | 5 | 5 | 5 | 5 | 5 | 5 | 5 | 4 | 0.3333 | 0.8759 | |
| | V.4 | 5 | 5 | 5 | 5 | 5 | 5 | 5 | 5 | 4 | 0.3333 | 0.8734 | |

¹When $l_{\min} = 5$, $S.9 = 4 < (l_{\min} = 5)$ as a result of condition of constraint: sum of synaptic effective ranges is constant=44 and reflects synaptic strength rebalance.

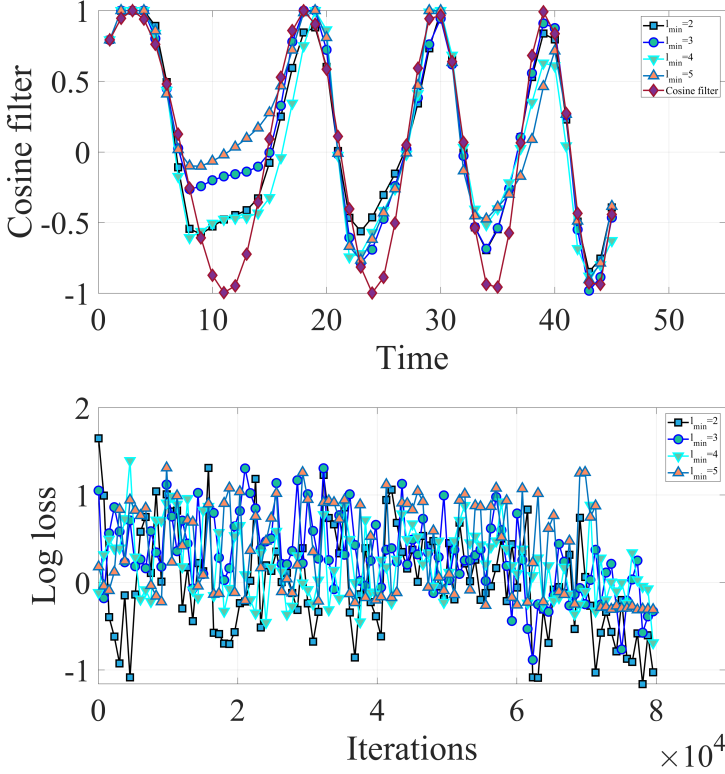


Fig. 13 ORPNN test results are $l_{\min} = 2 - 5$ and $k_{\max} = 9$ respectively. (e)ORPNN-MF(P&N)

Table 2 Synaptic effective range with different l_{\min} and different variables-brain plasticity ORPNN, test results are $l_{\min} = 2 - 5$ and $k_{\max} = 9$ respectively

| | V.L. | S.L. | | | | | | | | | Std | correlation coefficients |
|----------------|------|------|------|------|------|----------|------|--------------------|--------|----------|----------------|--------------------------|
| | | S.1 | S.2 | S.3 | S.4 | S.5 | S.6 | S.7 | S.8 | S.9 | | |
| $l_{\min} = 2$ | V.1 | 2332 | 2222 | 4444 | 3333 | 4544 | 3333 | 12141311 | 85913 | 6532 | 4.1366 | 0.8694 |
| | V.2 | 2323 | 2222 | 5555 | 4555 | 6676 | 2232 | 58108 | 9945 | 6448 | 2.2608 | 0.8694 |
| | V.3 | 2222 | 3333 | 5556 | 4334 | 3333 | 3333 | 98811 | 79109 | 8873 | 3.1402 | 0.8694^3 |
| | V.4 | 2222 | 3444 | 5333 | 2222 | 3333 | 5555 | 11131212 | 76310 | 86103 | 3.6209 | 0.8730 |
| $l_{\min} = 3$ | V.1 | 4444 | 4444 | 5455 | 4344 | 3333 | 9799 | 4444 | 5855 | 6766 | 1.7638 | 0.9282 |
| | V.2 | 4455 | 4455 | 3344 | 3344 | 4444 | 3344 | 8655 | 791010 | 8833 | 2.0276 | 0.9282 |
| | V.3 | 3333 | 5455 | 4344 | 4444 | 3344 | 4444 | 61166 ² | 6666 | 9688 | 1.5366 | 0.9282 |
| | V.4 | 3333 | 3333 | 4433 | 4334 | 3445 | 4445 | 4444 | 4444 | 13151613 | 3.1402 | 0.9282^3 |
| $l_{\min} = 4$ | V.1 | 4444 | 5555 | 6666 | 5555 | 5555 | 4444 | 5555 | 5555 | 5555 | 0.6009 | 0.8846 |
| | V.2 | 4444 | 5555 | 5555 | 4444 | 10101010 | 4444 | 4444 | 4444 | 4444 | 1.9650 | 0.8846 |
| | V.3 | 5555 | 5555 | 5555 | 5555 | 5555 | 5555 | 5555 | 5555 | 4444 | 0.3333 | 0.8846 |
| | V.4 | 5555 | 5555 | 4444 | 4444 | 6666 | 5555 | 5555 | 5555 | 5555 | 0.6009 | 0.8846^3 |
| $l_{\min} = 5$ | V.1 | 5 | 5 | 5 | 5 | 5 | 5 | 5 | 5 | 5 | 4 ¹ | 0.8579 |
| | V.2 | 5 | 5 | 5 | 5 | 5 | 5 | 5 | 5 | 5 | 4 | 0.3333 |
| | V.3 | 5 | 5 | 5 | 5 | 5 | 5 | 5 | 5 | 5 | 4 | 0.3333 |
| | V.4 | 5 | 5 | 5 | 5 | 5 | 5 | 5 | 5 | 5 | 4 | 0.3333 |

²We discovered the synaptic effective ranges are larger at local, resulting in the alignment of other synaptic effective ranges.

³Vanishing Gradients

Table 3 Synaptic effective range with different l_{\min} and different variables-brain plasticity ORPNN-PF, test results are $l_{\min} = 2 - 5$ and $k_{\max} = 9$ respectively

| | S.L. | | S.1 | S.2 | S.3 | S.4 | S.5 | S.6 | S.7 | S.8 | S.9 | Std | correlation coefficients |
|----------------|------|--|------|------|------|------|------|------|------|------|----------------|--------|--------------------------|
| | V.L. | | | | | | | | | | | | |
| $l_{\min} = 2$ | V.1 | | 3433 | 4444 | 5444 | 6666 | 7777 | 6666 | 3333 | 6666 | 4455 | 1.4530 | 0.9472 |
| | V.2 | | 7677 | 4444 | 7777 | 4444 | 6556 | 5444 | 4444 | 4544 | 3554 | 1.3642 | 0.9472 |
| | V.3 | | 3222 | 6666 | 5555 | 5555 | 7777 | 6666 | 4555 | 4444 | 4444 | 1.4530 | 0.9497 |
| | V.4 | | 3333 | 4444 | 6777 | 5555 | 5444 | 5555 | 7777 | 5566 | 4433 | 1.5366 | 0.9527 |
| $l_{\min} = 3$ | V.1 | | 4444 | 4444 | 6666 | 6677 | 5555 | 6666 | 4444 | 5555 | 4433 | 1.2693 | 0.9672 |
| | V.2 | | 4444 | 4544 | 5555 | 6555 | 5555 | 5555 | 6666 | 4455 | 6600 | 0.6009 | 0.9686 |
| | V.3 | | 6666 | 4444 | 4444 | 5555 | 5555 | 6666 | 5555 | 5555 | 4444 | 0.7817 | 0.9681 |
| | V.4 | | 4444 | 4544 | 4444 | 6366 | 6666 | 5555 | 5655 | 5555 | 5655 | 0.7817 | 0.9700 |
| $l_{\min} = 4$ | V.1 | | 5555 | 4444 | 5555 | 6666 | 5555 | 4444 | 4555 | 6566 | 5544 | 0.7817 | 0.9218 |
| | V.2 | | 5555 | 5555 | 5555 | 5555 | 4555 | 5555 | 5555 | 5555 | 5444 | 0.3333 | 0.9218 |
| | V.3 | | 5555 | 5555 | 6666 | 5555 | 5555 | 4444 | 4444 | 5555 | 5555 | 0.6009 | 0.9218 |
| | V.4 | | 4444 | 5555 | 4444 | 5555 | 6666 | 5555 | 5555 | 4454 | 6656 | 0.7817 | 0.9326 |
| $l_{\min} = 5$ | V.1 | | 5 | 5 | 5 | 5 | 5 | 5 | 5 | 5 | 4 ¹ | 0.3333 | 0.8991 |
| | V.2 | | 5 | 5 | 5 | 5 | 5 | 5 | 5 | 5 | 4 | 0.3333 | 0.8991 |
| | V.3 | | 5 | 5 | 5 | 5 | 5 | 5 | 5 | 5 | 4 | 0.3333 | 0.8991 |
| | V.4 | | 5 | 5 | 5 | 5 | 5 | 5 | 5 | 5 | 4 | 0.3333 | 0.8992 |

Table 4 Synaptic effective range with different l_{\min} and different variables-brain plasticity ORPNN-MF(P), test results are $l_{\min} = 2 - 5$ and $k_{\max} = 9$ respectively

| | S.L. | | S.1 | S.2 | S.3 | S.4 | S.5 | S.6 | S.7 | S.8 | S.9 | Std | correlation coefficients |
|----------------|------|--|------|------|------|------|------|------|------|------|----------------|--------|--------------------------|
| | V.L. | | | | | | | | | | | | |
| $l_{\min} = 2$ | V.1 | | 7777 | 4444 | 4444 | 4444 | 5555 | 4444 | 6666 | 5555 | 5555 | 1.0541 | 0.9194 |
| | V.2 | | 5555 | 4444 | 5555 | 6666 | 4444 | 4444 | 7777 | 5555 | 4444 | 1.0541 | 0.9350 |
| | V.3 | | 5555 | 4444 | 5555 | 7777 | 6666 | 4444 | 4444 | 5555 | 4444 | 1.0541 | 0.9302 |
| | V.4 | | 6666 | 6666 | 4444 | 4444 | 4444 | 4444 | 7777 | 4444 | 5555 | 1.1667 | 0.9382 |
| $l_{\min} = 3$ | V.1 | | 5555 | 4444 | 4444 | 6666 | 6666 | 5555 | 5555 | 5555 | 4444 | 0.7817 | 0.9188 |
| | V.2 | | 5555 | 5555 | 5555 | 5555 | 4444 | 5555 | 5555 | 5555 | 3333 | 0.3333 | 0.9352 |
| | V.3 | | 5555 | 5555 | 4444 | 6666 | 5555 | 4444 | 4444 | 6666 | 5555 | 0.7817 | 0.9335 |
| | V.4 | | 4444 | 4444 | 5555 | 5555 | 5555 | 6666 | 5555 | 5555 | 5555 | 0.6009 | 0.9265 |
| $l_{\min} = 4$ | V.1 | | 5555 | 5555 | 5555 | 5555 | 5555 | 5555 | 5555 | 5555 | 4444 | 0.3333 | 0.8991 |
| | V.2 | | 5555 | 4444 | 5555 | 5555 | 5555 | 5555 | 5555 | 5555 | 4444 | 0.3333 | 0.9073 |
| | V.3 | | 5555 | 5555 | 5555 | 5555 | 5555 | 4444 | 5555 | 5555 | 5555 | 0.3333 | 0.9117 |
| | V.4 | | 5555 | 5555 | 5555 | 5555 | 4444 | 5555 | 5555 | 5555 | 5555 | 0.3333 | 0.9115 |
| $l_{\min} = 5$ | V.1 | | 5 | 5 | 5 | 5 | 5 | 5 | 5 | 5 | 4 ¹ | 0.3333 | 0.8206 |
| | V.2 | | 5 | 5 | 5 | 5 | 5 | 5 | 5 | 5 | 4 | 0.3333 | 0.8278 |
| | V.3 | | 5 | 5 | 5 | 5 | 5 | 5 | 5 | 5 | 4 | 0.3333 | 0.8738 |
| | V.4 | | 5 | 5 | 5 | 5 | 5 | 5 | 5 | 5 | 4 | 0.3333 | 0.8663 |

Table 5 Synaptic effective range with different l_{\min} and different variables-brain plasticity ORPNN-MF(P&N), test results are $l_{\min} = 2 - 5$ and $k_{\max} = 9$ respectively

| | S.L. | | S.1 | S.2 | S.3 | S.4 | S.5 | S.6 | S.7 | S.8 | S.9 | Std | correlation coefficients |
|----------------|------|--|------|------|------|------|------|------|------|------|----------------|--------|--------------------------|
| | V.L. | | | | | | | | | | | | |
| $l_{\min} = 2$ | V.1 | | 5555 | 6664 | 3433 | 6666 | 4444 | 5444 | 6355 | 6666 | 3657 | 1.2693 | 0.9417 |
| | V.2 | | 3433 | 7666 | 3555 | 6565 | 6555 | 6566 | 5555 | 3533 | 5456 | 1.1667 | 0.9650 |
| | V.3 | | 5566 | 6545 | 5656 | 6653 | 5556 | 5556 | 6666 | 3333 | 3353 | 1.4530 | 0.9650 |
| | V.4 | | 4566 | 5555 | 3333 | 6666 | 5655 | 5655 | 5555 | 5555 | 6444 | 0.9280 | 0.9592 |
| $l_{\min} = 3$ | V.1 | | 5555 | 5655 | 6665 | 6555 | 4565 | 5555 | 4444 | 5445 | 4445 | 0.3333 | 0.9359 |
| | V.2 | | 5666 | 5666 | 5444 | 5555 | 5545 | 6666 | 4444 | 4555 | 5343 | 1.0541 | 0.9415 |
| | V.3 | | 5334 | 5555 | 5666 | 5555 | 5555 | 4665 | 5555 | 5555 | 5444 | 0.6009 | 0.9415 |
| | V.4 | | 5355 | 5655 | 4544 | 5655 | 4445 | 5555 | 5555 | 5555 | 5655 | 0.3333 | 0.9423 |
| $l_{\min} = 4$ | V.1 | | 5555 | 5555 | 5555 | 5445 | 5555 | 5555 | 5555 | 5555 | 4554 | 0.3333 | 0.9068 |
| | V.2 | | 5555 | 5555 | 5555 | 5555 | 5555 | 5555 | 5555 | 5555 | 4444 | 0.3333 | 0.9068 |
| | V.3 | | 5555 | 5555 | 5555 | 5555 | 5555 | 5555 | 5555 | 5555 | 4444 | 0.3333 | 0.9068 |
| | V.4 | | 5665 | 5555 | 5544 | 5555 | 5555 | 5555 | 5555 | 5555 | 4345 | 0.3333 | 0.9228 |
| $l_{\min} = 5$ | V.1 | | 5 | 5 | 5 | 5 | 5 | 5 | 5 | 5 | 4 ¹ | 0.3333 | 0.8894 |
| | V.2 | | 5 | 5 | 5 | 5 | 5 | 5 | 5 | 5 | 4 | 0.3333 | 0.8894 |
| | V.3 | | 5 | 5 | 5 | 5 | 5 | 5 | 5 | 5 | 4 | 0.3333 | 0.8894 |
| | V.4 | | 5 | 5 | 5 | 5 | 5 | 5 | 5 | 5 | 4 | 0.3333 | 0.8878 |

4 A simple PNN

A simple PNN, only correlation coefficient and astrocytes phagocytose synapses are considered rather than gradients update. Here, the PNN is simplified to only consider the astrocytes phagocytose synapses formula (4) with updated synaptic effective range weight and formula (1) with updated shared connection weight.

Two approaches are proposed: one approach is to evaluate the $f(t)$ and $h(t)$ correlation coefficient of $r(m, k)$ corresponding to the time range, each variable and synaptic position corresponding to one time range t and $t \in [n_3(m, k), n_3(m, k + 1)]$, and then considering whether or not to cancel the update of the previous-generation $r(m, k)$ depending on whether current correlation coefficient is improved compared to the previous generation; the other approach favors not processing $r(m, k)$ at all.

By comparing Table.6-7 and Fig.14-15, the first approach garners better simulation results, and the processing helps activate the synaptic effective range that varies with iteration.

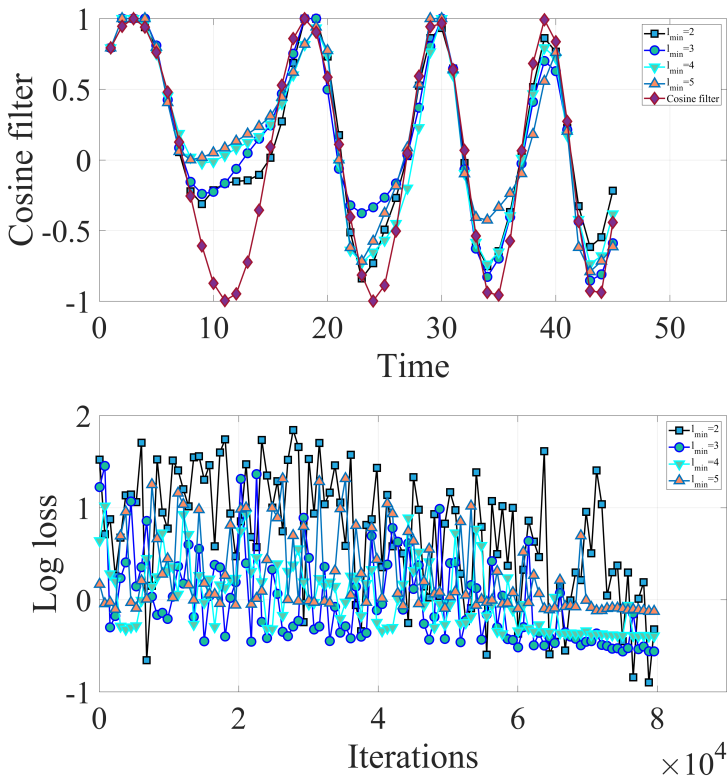


Fig. 14 simple ORPNN-PF without correlation coefficient correction, test results are $l_{\min} = 2 - 5$ and $k_{\max} = 9$ respectively.

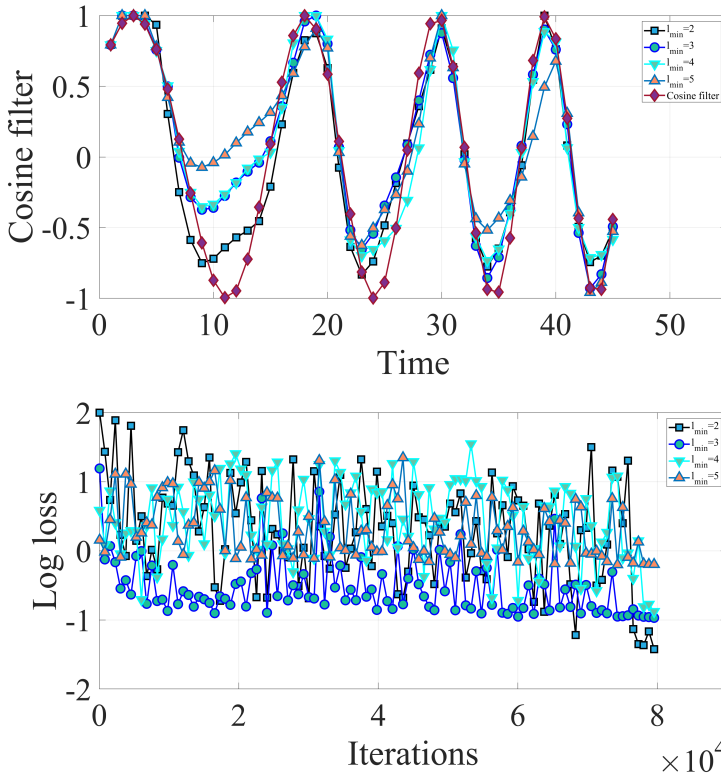


Fig. 15 simple ORPNN-PF with correlation coefficient correction, test results are $l_{\min} = 2 - 5$ and $k_{\max} = 9$ respectively.

Table 6 Synaptic effective range with different l_{\min} and different variables-brain plasticity simple ORPNN-PF without correlation coefficient correction, test results are $l_{\min} = 2 - 5$ and $k_{\max} = 9$ respectively

| | V.L. | S.L. | S.1 | S.2 | S.3 | S.4 | S.5 | S.6 | S.7 | S.8 | S.9 | Std | correlation coefficients |
|----------------|------|------|------|------|------|------|------|------|------|------|----------------|--------|--------------------------|
| $l_{\min} = 2$ | V.1 | | 5555 | 4444 | 4333 | 5444 | 7777 | 4444 | 6666 | 4445 | 5776 | 1.2693 | 0.9404 |
| | V.2 | | 3333 | 3333 | 4444 | 5555 | 6666 | 9999 | 4444 | 6666 | 4444 | 1.9003 | 0.9473 |
| | V.3 | | 5444 | 3333 | 3333 | 4444 | 7887 | 6555 | 4434 | 8666 | 4788 | 1.7638 | 0.9542 |
| | V.4 | | 3333 | 5444 | 5444 | 5555 | 6555 | 5555 | 5555 | 7888 | 3555 | 1.3642 | 0.9525 |
| $l_{\min} = 3$ | V.1 | | 6666 | 4444 | 6666 | 5555 | 5555 | 3444 | 5555 | 6666 | 4333 | 1.0541 | 0.9235 |
| | V.2 | | 7666 | 4444 | 4444 | 5555 | 4444 | 4444 | 6666 | 6655 | 4566 | 0.9280 | 0.9235 |
| | V.3 | | 6666 | 6666 | 4444 | 6666 | 5555 | 5555 | 4444 | 4444 | 4444 | 0.9280 | 0.9235 |
| | V.4 | | 5555 | 5555 | 5555 | 4444 | 5555 | 5555 | 6666 | 5555 | 4444 | 0.6009 | 0.9217 |
| $l_{\min} = 4$ | V.1 | | 4444 | 5555 | 5555 | 5555 | 6466 | 5555 | 4444 | 6666 | 4644 | 0.7817 | 0.8947 |
| | V.2 | | 5555 | 5555 | 5555 | 5555 | 4444 | 5555 | 5555 | 4444 | 6666 | 0.6009 | 0.9084 |
| | V.3 | | 6666 | 5555 | 5555 | 5555 | 4444 | 4555 | 6655 | 5555 | 4344 | 0.6009 | 0.9005 |
| | V.4 | | 5555 | 4444 | 5555 | 6566 | 4544 | 5555 | 5555 | 5555 | 5555 | 0.6009 | 0.8975 |
| $l_{\min} = 5$ | V.1 | | 5 | 5 | 5 | 5 | 5 | 5 | 5 | 5 | 4 ¹ | 0.3333 | 0.8671 |
| | V.2 | | 5 | 5 | 5 | 5 | 5 | 5 | 5 | 5 | 4 | 0.3333 | 0.8671 |
| | V.3 | | 5 | 5 | 5 | 5 | 5 | 5 | 5 | 5 | 4 | 0.3333 | 0.8671 |
| | V.4 | | 5 | 5 | 5 | 5 | 5 | 5 | 5 | 5 | 4 | 0.3333 | 0.8671 |

Table 7 Synaptic effective range with different l_{\min} and different variables-brain plasticity simple ORPNN-PF with correlation coefficient correction, test results are $l_{\min} = 2 - 5$ and $k_{\max} = 9$ respectively

| | S.L. | | S.1 | S.2 | S.3 | S.4 | S.5 | S.6 | S.7 | S.8 | S.9 | Std | correlation coefficients |
|----------------|------|--|------|------|------|------|------|------|------|------|----------------|--------|--------------------------|
| | V.L. | | | | | | | | | | | | |
| $l_{\min} = 2$ | V.1 | | 2333 | 7777 | 7888 | 6544 | 5666 | 4454 | 3333 | 4444 | 6445 | 1.7638 | 0.9427 |
| | V.2 | | 6666 | 3333 | 6566 | 6667 | 3333 | 4666 | 5454 | 7333 | 4866 | 1.6159 | 0.9545 |
| | V.3 | | 5444 | 4455 | 4333 | 6888 | 4443 | 5444 | 5746 | 4544 | 7587 | 1.7638 | 0.9545 |
| | V.4 | | 4333 | 4444 | 6777 | 4666 | 9777 | 3333 | 5455 | 4433 | 5666 | 1.6915 | 0.9622 |
| $l_{\min} = 3$ | V.1 | | 5555 | 4444 | 6666 | 6666 | 5555 | 5555 | 5545 | 4444 | 4454 | 0.7817 | 0.9451 |
| | V.2 | | 5555 | 6666 | 4554 | 5555 | 4333 | 5666 | 5555 | 4444 | 6556 | 1.0541 | 0.9451 |
| | V.3 | | 6666 | 4444 | 5555 | 6666 | 4444 | 3333 | 6666 | 4444 | 6666 | 1.1667 | 0.9451 |
| | V.4 | | 4444 | 5555 | 5555 | 6666 | 5555 | 5555 | 5555 | 5555 | 4444 | 0.6009 | 0.9488 |
| $l_{\min} = 4$ | V.1 | | 5655 | 5444 | 5555 | 5444 | 4444 | 4555 | 5555 | 6666 | 3566 | 0.7817 | 0.9288 |
| | V.2 | | 5555 | 5555 | 7877 | 5444 | 5555 | 4455 | 5444 | 4444 | 4555 | 0.9280 | 0.9368 |
| | V.3 | | 6666 | 4444 | 6666 | 4444 | 5555 | 4444 | 5555 | 5555 | 5555 | 0.7817 | 0.9261 |
| | V.4 | | 4444 | 7777 | 5444 | 5555 | 4444 | 5555 | 5555 | 5555 | 5555 | 0.9280 | 0.9364 |
| $l_{\min} = 5$ | V.1 | | 5 | 5 | 5 | 5 | 5 | 5 | 5 | 5 | 4 ¹ | 0.3333 | 0.8632 |
| | V.2 | | 5 | 5 | 5 | 5 | 5 | 5 | 5 | 5 | 4 | 0.3333 | 0.8632 |
| | V.3 | | 5 | 5 | 5 | 5 | 5 | 5 | 5 | 5 | 4 | 0.3333 | 0.8851 |
| | V.4 | | 5 | 5 | 5 | 5 | 5 | 5 | 5 | 5 | 4 | 0.3333 | 0.8728 |

5 Mechanism, Interpretability, Findings and Hypotheses

In addition to the shared weights of synaptic connections, we proposed a new Neural Network that includes weights of synaptic ranges for Forward propagation and Back propagation. And it gave a unified model of brain plasticity and synapse formation, and explains the mechanism of brain. And using more simulations to compare with the experiments which RNN cannot be achieved [14–27].

The mechanism of PNN enables the appropriate synapse to change the effective range for dendrite morphogenesis at critical period. When one synapse transfers a signal from one neuron to other with a better stimulation signal, PNN will change the current synaptic effective range based on Mean Squared Error (MSE) of loss function, with reference to current and memory brain plasticity, current gradient informational and memory positive and negative gradient informational synapse formation, and vice versa for the same reason.

In terms of the infectious disease dynamics, the infection rates of primitive strains and Delta strains varies in different time ranges, and the time interval corresponding to the cure rate will not be in line with the time interval corresponding to the infection rate, nor will the cure rate correspond exactly to the synaptic effective range effect of the infection rate, due to its high dependence on the medical condition.

Explaining in terms of synaptic competition, PNN is well-positioned to calculate the time ranges corresponding to the cure and infection rates, i.e., the synaptic effective ranges, through data processing, and then obtain the appropriate cure and infection rates, i.e., the shared weights of synaptic connections. During the emergency and non-emergency phase, i.e., critical period and closure of critical period, astrocytic effect is similar to government policies such as lockdown and mask rules, thereby affecting infection rate, cure rate and time ranges corresponding to them.

The optimization of synaptic effective range is also similar to the Residual Neural Network (ResNet)[12], as more layers don't necessarily perform better in training than fewer layers, and the number of layers is determined by training the synaptic effective range by gradient update with iterations.

By previous discussion's comparisons, we can summarize as follows:

PNN considers synaptic strength balance in dynamic of phagocytosing of synapses and static of constant sum of synapses length, it implements rebalancing strength between synapses[14]. From input to output units, neurons go through hidden layers, and when the lead synaptic effective range changes at critical period, these neurons, like a school of fish, also affect the postsynaptic neurons.

Synapse formation will inhibit dendrites generation to a certain extent in experiments, by simulations synapse formation will inhibit the function of dendrites such as receiving signals then affecting cognition [15]. The effects

of phagocytosing of synapses also help to synaptic growth. Because of rebalancing of synaptic strength, the phagocytosing of synapses makes neighboring synapses easily to grow. High IQ will have more neurons and their actions process fast, but synapse formation will inhabit those. Because of the rebalancing strength from input to output units, synapse formation leads to less neurons, and longer distance between neurons causes processing slower.

The Alcino J Silva's team suggested that memory ensembles by a retrograde mechanism [16]. Our research gave retrograde formula in preprint arXiv:2203.11740 version 1, it used memory gradient of the best previous synaptic effective range weight to update current gradient of synaptic effective range weight, it employs the retrograde mechanism, the memory best previous gradient is positive, and current gradient is negative. Memory gradient of the best previous synaptic effective range weight may be stored in the memory engram cells. And preprint version 2, it makes more sense the best previous memory retrieval process employs a retrograde mechanism through derivation of formula. The preprint version 3 considered the memory relatively inferior gradient of synaptic effective range weight by a retrograde mechanism.

The Alvarez-Buylla's lab proposed that human hippocampal neurogenesis drops sharply in children to undetectable levels in adults [17]. While PNN's simulations consider synapse formation, synapse formation leads to the decrease of neurogenesis, through the process from infancy to the senile phase.

But another study claimed human hippocampal neurogenesis persists throughout aging [18]. We guess if it may activate a new and longer circuit (a larger l_{\max}) in late iteration, even if synapse formation happens then decrease of neurons in early iteration, so a new circuit may lead to neurogenesis persists and may increase neurons in senile phase.

Closing the critical period (Such as astrocytic cortex memory persistence or astrocytes phagocytose synapses at critical period) will cause neurological disorder in experiments, but worse results in PNN simulations [19].

The cortex memory positive and negative synapse formation formula which considers gradient information of retrograde circuit, although it has same effects like astrocytes phagocytose synapses in simulation comparing with experiments. The cortex memory persistence gradient information of retrograde circuit similar to the Enforcing Resilience in a Spring Boot, in addition to considering the memory brain plasticity of architecture. The relatively good and inferior gradient information in synapse formation of retrograde circuit like the folds of the brain. Only considering positive (best previous gradient information) cortex memory persistence in simulation will inhibit synapse length changes with iterations. The memory of fear learning (or negative memory) can activate Synapses and observed obviously. By simulations, the PNN gave the two cases with and without negative memories. The brain plasticity was much easier to restore without negative memories, and the paper proposed $\alpha 7$ -nAChR-dependent astrocytic responsiveness is an integral part of the cellular substrate underlying memory persistence by impairing fear memory [20].

Astrocytes phagocytose synapses will avoid the local accumulation of synapses by simulation (Lack of astrocytes phagocytose synapses causes excitatory synapses and functionally impaired synapses accumulate in experiments and lead to destruction of cognition, but local longer synapses and worse results in PNN simulations) [21].

The brain cortex may be the space-time accumulation of the loss function. And the thicker cortex and more diverse individuals in brain may have high IQ in simulations and experiments [22].

The weights of synaptic ranges' memory negative and positive gradient information (or memory relatively good or inferior gradient information) is not memory brain plasticity, it used stimulus information to update brain plasticity. The stimulus information may be stored in the memory engram cells for inhibiting and inducing synapses and updating synaptic strength [23].

Based on principles of Optics, the relatively good or inferior gradient information's location is near the core of lens, and signals from input to output units with smaller losses go through core of lens. So different cortexes' relatively good and inferior gradient information is stimulated by stronger signals. And the relatively good or inferior gradient information may reflect improved memory retrieval process. And paper found that 1064-nm Transcranial photobiomodulation (tPBM) applied to the right prefrontal cortex (PFC) improves visual working memory capacity [24]. The effects of PNN memory structure and tPBM longer wavelengths may be the same, powerful penetrability of signals for improving memory capacity. It means signals go through easily neighboring areas of focus on convex or concave lens.

The Trinity College Institute of Neuroscience's findings may have witnessed entanglement mediated by consciousness-related brain functions, the consciousness-related or electrophysiological signals are unknown in NMR. Those brain functions must then operate non-classically, which would mean that consciousness is non-classical [25]. So PNN introduces exacted memory brain plasticity by quantum computing, and affects global brain, at hippocampus. At different cortices, but normal computing in details by Deep learning, Gradient Method and Statistics in gradient of synaptic connections, gradient of effective ranges, astrocytic cortex memory persistence by memory engram cells, astrocytes phagocytose synapses, different types neurons and synapses.

Priya Rajasethupathy research group of Rockefeller University shows that anteromedial thalamus selects strong memories and connects with cortex to selectively stabilize memories at remote time [26]. Refer to formula (2) and (4), working memory or short-term memory is consolidated and turns long-term memory. And we suggest strong and high flow working memory or short-term memory means maximum of directional derivatives of exacted memory brain plasticity is relatively good or inferior gradient of memory brain plasticity, means long-term memory.

Fast, efficient information transfer recently shown in functional magnetic resonance imaging (fMRI) with high spatial resolution, turbulence shows to

offer a based way to facilitate energy and information transfer across spatiotemporal scales in brain dynamics [27]. Memory from hippocampus to different cortices because of turbulence rather than laminar flow. Long-term memory is gradient of brain plasticity $\frac{\partial r}{\partial n}$ which is too idealistic, there is an angle $\alpha_c = \tan^{-1} \frac{\frac{\partial r}{\partial n}}{\frac{\partial r}{\partial t}}$, α_c will increase because of human aging, and turbulence becomes laminar flow gradually throughout aging, and smaller value tangent vector $\frac{\partial r}{\partial t}$ might impair to human intelligence.

Melanin-concentrating hormone decreases synaptic strength and modulates firing rate homeostasis. The paper’s findings identify the MCH (Melanin-concentrating hormone) system as vulnerable in early AD. MCH neurons are prominently active during REM (rapid eye movement) sleep. They find that a reduction in the percentage of active MCH neurons in App^{NL-G-F} mice is paralleled by a decrease in the time spent in REM sleep. Homeostatic plasticity response counteracts increased excitatory drive to CA1 pyramidal neurons in App^{NL-G-F} mice. Melanin-concentrating hormone reverses increased excitatory drive in App^{NL-G-F} CA1. Paper’s work suggests a model in which impaired MCH-dependent synaptic function in CA1 and perturbed REM sleep synergistically compromise neuronal homeostasis, contributing to aberrant neuronal activity in CA1[28]. It can be explained by the possible mechanism of AD, reverse turbulence relates to analyses of MCH, that synapses that should be decreased strength become excitatory, and should be increased strength become inhibitory.

We also hypothesized that heart failure affected the hippocampus. Like a water pump, the ability to pump and release water are weakened, making the radius of the large middle artery and the large middle aqueduct in the brain, turn to smaller, which may lead to Alzheimer’s disease.

We see that formula (2), $-g_r(m, k)$ are synaptic updates in the cortex, and $MW_1 \times g_r(m, k)_{best} + MW_2 \times g_r(m, k)_{worse} + MW_3 \times g_r(m, k)_{better}$ are from the upstream brain regions cortical memory engrams.

For memory engrams in the cortex, because reverse turbulence conjecture makes the gradient that updates the synaptic effective range weight take a positive gradient, resulting in synaptic loss, synaptic inhibition excitation reversal, forward and backward memory loss makes the memory engrams smoothing, and neuroinflammation.

A healthy brain transcerebral regions retrieves memory engrams in the upstream brain regions through a retrograde mechanism, and the ensembles of these memory engrams through smaller upstream aqueducts to larger downstream aqueducts does not have to meet the critical conditions of turbulence.

For the memory engrams of other cortices obtained across brain regions, due to the reverse turbulence, the cortex should be retrograde to obtain the memory engrams of the upstream brain regions cortexes without obtaining causes neurons to be lost, or difficulty in obtaining at early stage of AD and causing amnesia, but more cortexes that obtain memory engrams in downstream brain regions cause redundant memory information leading to

hallucinations, while more emotional memories in downstream brain regions, which will make people irritable and depressed. Moreover, reverse turbulence makes the emotional memory retrograde transmission to the upstream brain regions, which will reduce the emotion of the downstream brain regions, and then the downstream brain regions and synapses lose activity, so the hippocampus and downstream brain regions become hard and accelerate brain aging.

The Heart-Brain Deep learning model considering intestine, liver and kidney function through the reverse turbulence of brain explains that the memory engrams of the upstream brain regions cannot be retrieved; Local cortex synapse loss; Inhibition and excitation of synapse reversal in the cortex, smoothing memory engrams because of blood disturbances; Extraction of redundant memory engrams in downstream brain regions caused hallucinations, irritability, depression; Neuroinflammation by lacking immune cells, high probability accompanied by atherosclerosis leading to systolic hypertension, high probability accompanied by cerebral infarction, high probability accompanied by heart failure; Gradual atrophy and hardening of the hippocampus, brain aging, circadian rhythm disorders, and cognitive impairment occurs as a result.

The flow turbulent of immune cells through the aqueducts between brain regions, reverse turbulence of immune cells can bring the opposite stimulating effect to microglia, which affect the direction of memory engrams because of the opposite stimulation, the reverse of memory engrams leads to memory loss and cognitive decline. According to our model, clearance of immune cells weakens microglial activation, it does help with delayed memory loss and cognitive decline, and cognitive search is changed from the correct negative gradient to the false positive gradient, but the cognitive search becomes a random search based on early memory engrams. Compared to clearing immune cells, it is also a good idea to possibly improve the turbulent flow of immune cells crossing between different brain regions.

The Reynolds number distinguishes whether the fluid flow is laminar or turbulent. The Reynolds number formula $Re = \rho v d / \mu$, where v , ρ and μ are the flow velocity, density and viscosity coefficient of the fluid, respectively, and d is a characteristic length. For example, if fluid flows through a circular pipe, d is the equivalent diameter of the pipe. If moderate exercise promotes arterial dilation and increase d , increases blood flow and increases v , prevents blood viscosity from decreasing μ . Moderate aerobic exercise increases the Raynaud number so that laminar flow between the aqueducts from downstream brain regions to upstream brain regions becomes turbulent, which can prevent Alzheimer's disease.

In addition, according to the above analysis of Intestine-Liver-Kidney-Heart-Brain model for Alzheimer's disease, we should consider drugs and foods that Sleep/Wake Regulation, drugs and foods that restore liver function, drugs and foods that restore kidney function, foods and drugs that improve intestinal probiotics, drugs and foods that prevent systolic hypertension caused by

atherosclerosis, drugs and foods that prevent cerebral infarction, drugs and foods that prevent heart failure, drugs and foods that prevent depression, drugs and foods to treat aging, drugs and foods that promote brain metabolism and aerobic exercise, which help remove garbage and toxins from cerebral arteries and aqueducts, which may be effective for early Alzheimer's disease.

We may be able to design Alzheimer's disease drugs based on this.

The 4 findings were as follows:

1. Astrocytic cortex memory persistence also inhibits local synaptic accumulation and excitation, and the model inspires experiments.
2. But the thickest cortex and the most diverse individuals in brain may have low IQ in simulation, so the PNN can guide the experiments, and experiments are special situations of models. And our guess is that more advanced cortexes near the core of brain.
3. It may be the process of astrocytes phagocytose synapses is driven by positive and negative memories of brain plasticity, based on $r(m, k) = r(m, k) + rand \times [MW_1 \times R + MW_2 \times Q_N + MW_3 \times Q_P - r(m, k)] + P$ in formula (4), because of the positive or negative value of Q_P or Q_N .
4. For PNN, the role of long-term memory is more pronounced than short-term memory.

The 4 hypotheses were as follows:

1. Negative or positive emotion and cognition reflect non-classical exacted memories brains plasticity by quantum mechanics, are short-term hippocampal memories. The wave function is high-frequency. And wave function of exacted memories brains plasticity shows kinetic energy because of high-speed particles, produce at hippocampus. By PNN, we propose these appeared barriers from hippocampus to different cortexes, wave function will lead to exponential decay, and wave function of high-frequency turns to low-frequency. At last, long-term stimulus information stored in memory engram cells of different cortexes. And long-term memories exhibit potential energy releases;

2. Barriers may relate to astrocytes;

3. Directional derivative of working memory will flow to the different cortices and stored in memory engram cells. High flow working memory or maximum of directional derivatives of working memory means gradient of short-term memory will turn to long-term memory.

4. In PNN simulations, ensembles of long-term memory produced once each iteration, so it occurs once at strong probability. but retrieval processes of short-term memory happened once by many iterations, and occurrences are poor probability.

6 Conclusion

- 1 Based on the RNN architecture, we accomplished the model construction, formula derivation and algorithm testing for PNN. We elucidated the mechanism of PNN based on the latest MIT research on synaptic strength rebalance, and also grounded our study on the basis of findings of the

Stanford research, which suggested that synapse formation is important for competition in dendrite morphogenesis. The effects of astrocyte impact on brain plasticity and synapse formation is an important mechanism of our Neural Network at critical period or the closure of critical period. In addition to formula (1) and (2), which is derived from Back Propagation and features the synaptic shared connection weight and the effective range weight respectively. We also managed to figure out synaptic competition by current gradient informational and memory positive and negative gradient informational synapse formation at critical period through formula (2), synaptic strength rebalance through formula (2) and (4), and current and memory brain plasticity at critical period through formula (4). Formula (4) through working memory, but Formula (2) through long-term memory. However, our Neural Network is no longer confined to the simple physical concept of synaptic strength rebalance - it treats synapses as a group of intelligent agents to achieve synaptic strength rebalance. The gradient method to update the synaptic effective range weights by long-term memory. The quantum computing to update the synaptic effective range weights by short-term memory. Short-term memory travels through the barriers of hippocampus and different cortices and turns into long-term memory.

- 2 The memory positive and negative gradient informational synapse formation needs to consider the forgotten memory-astrocytic synapse formation cortex memory persistence factor. Memory brain plasticity involves plus or minus disturbance- astrocytes phagocytose synapses factor, thus enabling dynamic synaptic strength balance. The effect of astrocyte made local synaptic effective range remain in an appropriate length at critical period. We give decreasing weights of factors at critical period. We try to deduce the mechanism of failure in brain plasticity by model at the closure of critical period in details by contrasting with previous studies. The simulation in Tables similar to that failure to the closure of critical period results in neurodevelopmental disorders[19]. The findings of our study proved meaningful, which revealed that much like astrocytes phagocytose synapses factor. The cortex memory persistence factor obtained by the simulation of the mathematical model also inhibits the local accumulation of synapses [21].
- 3 Test results of the 3 scenarios all concern the memory best previous solution. All the PNNs with gradient-optimized synaptic effective range fared better than those with random synaptic effective range, which in turn outperformed PNNs with constant synaptic effective range. Constant synaptic effective range is achieved when the minimum synaptic effective range grows to coincide with the maximum synaptic effective range, which usually takes place in the cognition of the senile phase. The iteration of CRPNN is difficult to convergence due to a lack of plasticity and diversity, and RRPNN demonstrates slow convergence in testing.
- 4 We believe our work is of profound significance for the development of NN research. Furthermore, PNN takes into account the memory positive and negative gradient informational synapse formation, and brain plasticity and

synapse formation change architecture of NN is a new method of Deep Learning. We can obtain better results in Tables of correlation coefficients respectively, when ORPNN contains both astrocytic synapse formation cortex memory persistence factor and astrocytes phagocytose synapses factor at critical period. Both the memory best previous gradient information, the relatively good gradient information and the relatively inferior gradient information are considered, which increases the activity of the synaptic effective range with iteration changes and thereby improves the simulation results. The relatively good and inferior gradient information in synapse formation of retrograde circuit like the folds of the brain [16]. And we discussed the relationship of human intelligence and cortical thickness, individual differences in brain by simulations and experiments, and PNN can guide the experiments, and experiments are special situations of models[22]. Our model PNN fits very well with the memory engram cells that strengthened synaptic strength [23]. The effects of PNN's memory structure and longer wavelengths of tPBM may be the same, powerful penetrability of signals for improving memory capacity [24].

- 5 In addition to the shared weights of synaptic connections, Forward propagation and Back propagation also include weights of synaptic ranges. We developed the concept of weights for NN and divided the weights into categories, namely weights of synaptic shared connection and effective range. The latter reflects synaptic competition, strength rebalance, current and memory brain plasticity and current gradient informational and memory negative and positive gradient informational synapse formation at critical period. From input to output units, they go through hidden layers, and when the lead synaptic effective range changes at critical period, these neurons, like a school of fish, also affect the postsynaptic neurons.
- 6 We also attempted to simulate PNN cognition process from infancy to the senile phase, and by analyzing relationship between different synapse formation and correlation coefficients. We may reasonably assume that the minimum synaptic effective range increases and synapse population decreases for synapse formation of senile phase.
- 7 In the next step of our study, we took the real pandemic data into consideration, and PNN may well be used to process the pandemic data of the original strain and the variant Delta strain, in an effort to optimize the time interval of the synaptic effective range, and then different connection weights will be applied for cure and infection rates. We will calculate the connection weights by PNN, and the synaptic effective range, based on which we then formulate contingency plans for different period.
- 8 By testing, we made a similar observation to that of Dr. Luo's team through PNN: synapse formation to a certain extent is detrimental to dendrites, and synapse formation leads to a reduction in changes of the synaptic effective range, therefore disrupting diversity and plasticity, including results considering cortex memory persistence factor and astrocytes phagocytose synapses factor separately.

- 9 The synaptic competition mechanism NN is suitable for RNN architecture as well as BP, and our next step is to conduct research on the implementation of synaptic competition, strength rebalance, memory generation, memory consolidation, memory loss and critical period by BP.
- 10 In simulation, if a same type of shared connection weight changes, all the weights of effective ranges may be consequently updated for better results.
- 11 To be honest, the effects of astrocyte affect on brain plasticity and synapse formation was inspired by Particle Swarm Optimization (PSO) [39] and consolidation of concrete, and critical period of brain plasticity really depends on inertia weight of PSO [40]. Only synapse formation affects on brain cognition refers biological tests of neuroscience [15], quantum computer of brain [25] and memory consolidation [26], but also is relevant to the FEM. Synaptic strength rebalance is actually inspired by the conservation of energy. The question we proposed is whether the promotion of computational neuroscience and brain cognition was achieved by model construction, formula derivation or algorithm testing, and whether we can reduce the number of animal experiments and their suffering through the guidance of model simulation planning. We resorted to the Artificial Neural Network (ANN), Evolutionary Computation and other numerical methods for hypotheses, possible explanations and rules, rather than only biological experiments.
- 12 In formula (2), the PNN gradient information considering both positive and negative memories outperforms the case where only positive memory is considered, and the synaptic effective range of the former is more active with iteration changes, yielding better optimization results.
- 13 We simplified the PNN to only consider the update of astrocytes phagocytose synapses rather than the gradient update, and decided whether to cancel the update of astrocytes phagocytose synapses based on the correlation coefficient corresponding to the time range between the current and previous generation, each variable and synaptic position corresponding to one time range. The model considering whether or not to cancel the phagocytic update which yields better simulation results than model not processing, and the synaptic effective range is more active with iterations.
- 14 Particle Swarm Optimization (PSO) considers the global optimal solution and the best previous solution to update the velocity of particles-2 parameters, and refers PNN can also introduce the relatively good and the relatively inferior solution to update the velocity of particle-4 parameters.
- 15 In formula (2) and (4), we suggest the PNN is not only a classical normal computer in synapse formation and brain plasticity, but also a non-classical quantum computer in working memory brain plasticity, in extracted relatively good or inferior memories brains plasticity will exhibits exponential decay of wave function for a while because of barriers. When you are considering one problem, whether positive or negative, the exacted memory brain plasticity reflects quantum.
- 16 The process of astrocytes phagocytose synapses may both have quantum computing and traditional computing, and may be the process is driven by

- positive and negative memories of brain plasticity, through interactions of excitatory and inhibitory transmitters.
- 17 The quantum entanglement between the heart and brain may be beyond absolute space-time. Non-classical working memories by quantum computing, are short-term memories, produce at hippocampus. The wave function is high-frequency, and shows kinetic energy. These appeared barriers from hippocampus to different cortices, wave function will lead to exponential decay. At last, long-term stimulus information stored in memory engram cells of different cortices, and memories exhibit potential energy. Barriers may relate to astrocytes. Directional derivative of working memory will flow to the different cortices and stored in memory engram cells. High flow working memory or maximum of directional derivatives of working memory means gradient of short-term memory will turn to long-term memory. From the hippocampus to different cortices, memory flow may be considered to be the transmission of the rate of change of the architecture. From the hippocampus to the first cortex, memory may mean Jacobian matrix of brain plasticity. From the first cortex to the second cortex, memory may be the second derivative of the brain plasticity. We also hypothesized that heart failure affected the forward and backward transmission of neurotransmitters.
 - 18 When $\alpha_c \geq \pi$, model of memory Generation-Consolidation-Loss tries to give the mechanism of Alzheimer's disease. The simultaneous interaction of two different turbulence directions of $\alpha_c \geq \pi$ memory loss and $\alpha_c \leq \frac{\pi}{2}$ memory consolidation leads to β -amyloid plaques in brain. Another explanation might be false positive gradient of Back-propagation of memory loss, it is also indirectly proved by the results of other's experiments [28]. We hypothesize the possible mechanism of Alzheimer's disease, and that brain β -amyloid plaques and tau protein may only be a symptom or not the main cause.
 - 19 We try to simulate the prefrontal lobe, amygdala, and hippocampus. Along the forward direction, the fear memory gradually increases. Along the direction of backpropagation, the optimization order increases.
 - 20 The first research to synaptic strength rebalance was achieved in Deep learning. The parameters of relatively inferior negative and relatively good memory were considered in Deep learning for the first time, and the parameters also enriched the research of particle swarm optimization and genetic algorithm. Studies first proposed that memory flow in each cortex of the brain must be greater than the critical value in order for laminar flow to become turbulent and spread to the upstream brain regions, the critical angle of turbulence is related to the mnemonic weight. Based on turbulence, the study gives that the flow of memory from the downstream brain regions to the upstream brain regions may be the transmission of the brain architecture rate of change, and the mnemonic architecture of the downstream first cortex is r_m , then the mnemonic architecture of the upstream n th cortex may be approximately the $n - 1$ th derivative of r_m , our memory may be a two-dimensional logarithmic spiral, in this way, the $n - 1$ th derivative of r_m is not much different from r_m , synaptic connection weight

or range weight is stored in a logarithmic spiral, a unique variable that angle as a logarithmic spiral. The study first showed that mnemonic architecture formula-logarithmic spiral, turbulent movement in brain regions is only energy loss and memory engrams are approximate. The study first showed that the upstream brain regions are more rational learning than the downstream brain regions and requires higher-order optimization, and the downstream brain regions have more negative memory, and the Deep learning model for upstream and downstream brain regions is given. The study considered the Deep learning model for upstream and downstream brain regions combined with reverse turbulence of downstream brain regions to explain 15 phenomena of Alzheimer's disease. The non-classical experiment with reference to the Heart-Brain interactions were studied, using wave function with exponential decay to update the Deep learning model of the synaptic effective range firstly. This explains the dynamics cause of shaping in the geometry of the brain, related to the turbulent movement of the logarithmic spiral of the brain.

Author contributions

Conceptualization, J.B.T., B.Q.S., Y.X., J.Q.L and C.W., Formal analysis, J.B.T., B.Q.S., W.D.Z., S.Y.Q., L.K.C., and Y.X., Funding acquisition, C.W., and B.Q.S.; Investigation, J.B.T., C.W., B.Q.S., L.K.C., Y.X., J.Q.L and S.Y.Q.; Methodology and Coding, J.B.T., Supervision, B.Q.S., Y.X., J.Q.L, C.W., S.Y.Q., and W.D.Z.; Writing-original draft, J.B.T., J.X.Z., and L.K.C.; Writing-review & editing, W.D.Z. B.Q.S., J.Q.L, L.K.C., and Y.X.; All authors have read and agreed to the published version of the manuscript.

Competing interests

The authors declare no competing interest

References

- [1] Rosenblatt, F. (1957) The Perceptron, a Perceiving and Recognizing Automaton Project Para. Cornell Aeronautical Laboratory.
- [2] Hopfield J J. Neural networks and physical systems with emergent collective computational abilities. Proceedings of the National Academy of Sciences of the United States of America, 1982, 79(8): 2554-2558.
- [3] Hinton, G. E. and Sejnowski, T. J. (1983) Optimal perceptual inference. Proceedings of the IEEE conference on Computer Vision and Pattern Recognition, Washington DC.
- [4] Rumelhart D E, Hinton G E, Williams R J. Learning representations by back-propagating errors. Nature, 1986, 323(6088): 533-536.

- [5] Fukushima K. Neocognitron: A self organizing neural network model for a mechanism of pattern recognition unaffected by shift in position. *Biological Cybernetics*, 1980, 36(4): 193-202.
- [6] Lecun Y, Boser B, Denker J S, et al. Backpropagation applied to handwritten zip code recognition. *Neural Computation*, 1989, 1(4): 541-551.
- [7] Maass W. Networks of spiking neurons: The third generation of neural network models. *Neural Networks*, 1997, 10(9): 1659-1671.
- [8] Hochreiter S, Schmidhuber J. Long short-term memory. *Neural Computation*. 1997 Nov 15;9(8):1735-80. doi: 10.1162/neco.1997.9.8.1735. PMID: 9377276.
- [9] Hinton G E, Osindero S, Teh Y W. A fast learning algorithm for deep belief nets. *Neural Computation*, 2006, 18(7): 1527-1554.
- [10] Krizhevsky A, Sutskever I, Hinton G E. Imagenet classification with deep convolutional neural networks. *Communications of the Acm*, 2017, 60(6): 84-90.
- [11] Z.-H. Zhou and J. Feng. Deep forest. *National Science Review*, 2019, 6(1): 74-86.
- [12] He K, Zhang X, Ren S, et al. Deep Residual Learning for Image Recognition[J]. *IEEE*, 2016.
- [13] Michael L. Littman, Ifeoma Ajunwa, Guy Berger, Craig Boutilier, Morgan Currie, Finale Doshi-Velez, Gillian Hadfield, Michael C. Horowitz, Charles Isbell, Hiroaki Kitano, Karen Levy, Terah Lyons, Melanie Mitchell, Julie Shah, Steven Sloman, Shannon Vallor, and Toby Walsh. "Gathering Strength, Gathering Storms: The One Hundred Year Study on Artificial Intelligence (AI100) 2021 Study Panel Report." Stanford University, Stanford, CA, September 2021. Doc: <http://ai100.stanford.edu/2021-report>. Accessed: September 16, 2021 .
- [14] El-Boustani, Sami et al. "Locally coordinated synaptic plasticity of visual cortex neurons in vivo." *Science (New York, N.Y.)* vol. 360,6395 (2018): 1349-1354. doi:10.1126/science.aao0862
- [15] Yukari H. Takeo et al. GluD2- and Cbln1-mediated competitive interactions shape the dendritic arbors of cerebellar Purkinje cells. *Neuron*, 2021, doi:10.1016/j.neuron.2020.11.028.
- [16] Lavi A, Sehgal M, de Sousa AF, Ter-Mkrtchyan D, Sisan F, Luchetti A, Okabe A, Bear C, Silva AJ. Local memory allocation recruits

- memory ensembles across brain regions. *Neuron*. 2022 Dec 15;S0896-6273(22)01072-8. doi: 10.1016/j.neuron.2022.11.018. Epub ahead of print. PMID: 36563678.
- [17] Sorrells SF, Paredes MF, Cebrian-Silla A, Sandoval K, Qi D, Kelley KW, James D, Mayer S, Chang J, Auguste KI, Chang EF, Gutierrez AJ, Kriegstein AR, Mathern GW, Oldham MC, Huang EJ, Garcia-Verdugo JM, Yang Z, Alvarez-Buylla A. Human hippocampal neurogenesis drops sharply in children to undetectable levels in adults. *Nature*. 2018 Mar 15;555(7696):377-381. doi: 10.1038/nature25975. Epub 2018 Mar 7. PMID: 29513649; PMCID: PMC6179355.
- [18] Boldrini M, Fulmore CA, Tartt AN, Simeon LR, Pavlova I, Poposka V, Rosoklija GB, Stankov A, Arango V, Dwork AJ, Hen R, Mann JJ. Human Hippocampal Neurogenesis Persists throughout Aging. *Cell Stem Cell*. 2018 Apr 5;22(4):589-599.e5. doi: 10.1016/j.stem.2018.03.015. PMID: 29625071; PMCID: PMC5957089. .
- [19] Ribot J, Breton R, Calvo CF, Moulard J, Ezan P, Zapata J, Samama K, Moreau M, Bemelmans AP, Sabatet V, Dingli F, Loew D, Milleret C, Billuart P, Dallérac G, Rouach N. Astrocytes close the mouse critical period for visual plasticity. *Science*. 2021 Jul 2;373(6550):77-81. doi: 10.1126/science.abf5273. PMID: 34210880.
- [20] Zhang, K., Förster, R., He, W. et al. Fear learning induces α 7-nicotinic acetylcholine receptor-mediated astrocytic responsiveness that is required for memory persistence. *Nat Neurosci* 24, 1686–1698 (2021). <https://doi.org/10.1038/s41593-021-00949-8>
- [21] Lee JH, Kim JY, Noh S, Lee H, Lee SY, Mun JY, Park H, Chung WS. Astrocytes phagocytose adult hippocampal synapses for circuit homeostasis. *Nature*. 2021 Feb;590(7847):612-617. doi: 10.1038/s41586-020-03060-3. Epub 2020 Dec 23. PMID: 33361813.
- [22] Galakhova AA, Hunt S, Wilbers R, Heyer DB, de Kock CPJ, Mansvelder HD, Goriounova NA. Evolution of cortical neurons supporting human cognition. *Trends Cogn Sci*. 2022 Nov;26(11):909-922. doi: 10.1016/j.tics.2022.08.012. Epub 2022 Sep 15. PMID: 36117080; PMCID: PMC9561064.
- [23] Ryan TJ, Roy DS, Pignatelli M, Arons A, Tonegawa S. Memory. Engram cells retain memory under retrograde amnesia. *Science*. 2015 May 29;348(6238):1007-13. doi: 10.1126/science.aaa5542. Epub 2015 May 28. PMID: 26023136; PMCID: PMC5583719.
- [24] Zhao C, Li D, Kong Y, Liu H, Hu Y, Niu H, Jensen O, Li X, Liu H, Song Y. Transcranial photobiomodulation enhances visual working

- memory capacity in humans. *Sci Adv.* 2022 Dec 2;8(48):eabq3211. doi: 10.1126/sciadv.abq3211. Epub 2022 Dec 2. PMID: 36459562.
- [25] Christian Matthias Kerskens, David López Pérez. Experimental indications of non-classical brain functions. *Journal of Physics Communications*, 2022, 6(10): 105001. DOI: 10.1088/2399-6528/ac94be.
- [26] Toader AC, Regalado JM, Li YR, Terceros A, Yadav N, Kumar S, Satow S, Hollunder F, Bonito-Oliva A, Rajasethupathy P. Anteromedial thalamus gates the selection and stabilization of long-term memories. *Cell.* 2023 Mar 30;186(7):1369-1381.e17. doi: 10.1016/j.cell.2023.02.024. PMID: 37001501.
- [27] Deco, G., Liebana Garcia, S., Sanz Perl, Y. et al. The effect of turbulence in brain dynamics information transfer measured with magnetoencephalography. *Commun Phys* 6, 74 (2023). <https://doi.org/10.1038/s42005-023-01192-2>.
- [28] Calafate, S., Özturan, G., Thrupp, N. et al. Early alterations in the MCH system link aberrant neuronal activity and sleep disturbances in a mouse model of Alzheimer’s disease. *Nat Neurosci* 26, 1021–1031 (2023). <https://doi.org/10.1038/s41593-023-01325-4>
- [29] Dou, H.-S., *Origin of Turbulence-Energy Gradient Theory*, 2022, Springer. <https://link.springer.com/book/10.1007/978-981-19-0087-7>.
- [30] Adema Ribic et al. Synapse-Selective Control of Cortical Maturation and Plasticity by Parvalbumin-Autonomous Action of SynCAM 1. *Cell Reports*, published online January 8, 2019; doi: 10.1016/j.celrep.2018.12.069.
- [31] R. M. Fitzsimonds, H. J. Song, M. M. Poo, Propagation of activity-dependent synaptic depression in simple neural networks. *Nature* 388, 439–448 (1997).
- [32] J. L. Du, M. M. Poo, Rapid BDNF-induced retrograde synaptic modification in a developing retinotectal system. *Nature* 429, 878–883 (2004).
- [33] J. L. Du, H. P. Wei, Z. R. Wang, S. T. Wong, M. M. Poo, Long-range retrograde spread of LTP and LTD from optic tectum to retina. *Proc. Natl. Acad. Sci. U.S.A.* 106, 18890–18896 (2009).
- [34] G. Bi, M. Poo, Synaptic modification by correlated activity: Hebb’s postulate revisited. *Annu. Rev. Neurosci.* 24, 139–166 (2001).
- [35] H.-Z. W. Tao, L. I. Zhang, G.-Q. Bi, M.-M. Poo, Selective presynaptic propagation of long-term potentiation in defined neural networks. *J. Neurosci.* 20, 3233–3243 (2000).

- [36] Bertens, P., Lee, SW. Network of evolvable neural units can learn synaptic learning rules and spiking dynamics. *Nat Mach Intell* ,2,791–799,(2020). doi:<https://doi.org/10.1038/s42256-020-00267-x>.
- [37] Yihan Wang, Qian-Quan Sun. A long-range, recurrent neuronal network linking the emotion regions with the somatic motor cortex, *Cell Reports*, published online september 21, 2021; 36, (2021). doi:<https://doi.org/10.1016/j.celrep.2021.109733>.
- [38] Suzuki K, Elegheert J, Song I, Sasakura H, Senkov O, Matsuda K, Kakegawa W, Clayton AJ, Chang VT, Ferrer-Ferrer M, Miura E, Kaushik R, Ikeno M, Morioka Y, Takeuchi Y, Shimada T, Otsuka S, Stoyanov S, Watanabe M, Takeuchi K, Dityatev A, Aricescu AR, Yuzaki M. A synthetic synaptic organizer protein restores glutamatergic neuronal circuits. *Science*. 2020 Aug 28;369(6507):eabb4853. doi: 10.1126/science.abb4853. PMID: 32855309; PMCID: PMC7116145.
- [39] Kennedy J . Particle swarm optimization[J]. *Proc. of 1995 IEEE Int. Conf. Neural Networks*, (Perth, Australia), Nov. 27-Dec. 2011, 4(8):1942-1948 vol.4.
- [40] Shi Y . A Modified Particle Swarm Optimizer[C]// *Proc of IEEE Icc Conference*. 1998.